23 The kinetics of complex reactions

Chain reactions

23.1 The rate laws of chain reactions

23.2 Explosions

Polymerization kinetics

23.3 Stepwise polymerization

23.4 Chain polymerization

Homogeneous catalysis

23.5 Features of homogeneous catalysis

23.6 Enzymes

Photochemistry

23.7 Kinetics of photophysical and photochemical processes

I23.1 Impact on environmental science: The chemistry of stratospheric ozone

I23.2 Impact on biochemistry: Harvesting of light during plant photosynthesis

23.8 Complex photochemical processes

I23.3 Impact on medicine: Photodynamic therapy

Checklist of key ideas

Further reading

Further information 23.1: The Förster theory of resonance energy transfer

Discussion questions

Exercises

Problems

This chapter extends the material introduced in Chapter 22 by showing how to deal with complex reaction mechanisms. First, we consider chain reactions and see that either complicated or simple rate laws can be obtained, depending on the conditions. Under certain circumstances, a chain reaction can become explosive, and we see some of the reasons for this behaviour. An important application of these more complicated techniques is to the kinetics of polymerization reactions. There are two major classes of polymerization process and the average molar mass of the product varies with time in distinctive ways. Second, we describe homogeneous catalysis and apply the associated concepts to enzyme-catalysed reactions. Finally, we describe the principles of photochemistry and apply them to problems in environmental science, biochemistry, and medicine.

Many reactions take place by mechanisms that involve several elementary steps. Some take place at a useful rate only after absorption of light or if a catalyst is present. In this chapter we see how to develop the ideas introduced in Chapter 22 to deal with these special kinds of reactions.

Chain reactions

Many gas-phase reactions and liquid-phase polymerization reactions are **chain reactions**. In a chain reaction, a reaction intermediate produced in one step generates an intermediate in a subsequent step, then that intermediate generates another intermediate, and so on. The intermediates in a chain reaction are called **chain carriers**. In a **radical chain reaction** the chain carriers are radicals (species with unpaired electrons). Ions may also act as chain carriers. In nuclear fission the chain carriers are neutrons.

23.1 The rate laws of chain reactions

A chain reaction can have a simple rate law. As a first example, consider the **pyrolysis**, or thermal decomposition in the absence of air, of acetaldehyde (ethanal, CH_3CHO), which is found to be three-halves order in CH_3CHO:

$$CH_3CHO(g) \rightarrow CH_4(g) + CO(g) \qquad v = k[CH_3CHO]^{3/2} \tag{23.1}$$

Some ethane is also detected. The **Rice–Herzfeld mechanism** for this reaction is as follows (the dot signifies an unpaired electron and marks a radical):

Initiation:	$CH_3CHO \rightarrow \cdot CH_3 + \cdot CHO$	$v = k_i[CH_3CHO]$
Propagation:	$CH_3CHO + \cdot CH_3 \rightarrow CH_3CO\cdot + CH_4$	$v = k_p[CH_3CHO][\cdot CH_3]$
Propagation:	$CH_3CO\cdot \rightarrow \cdot CH_3 + CO$	$v = k'_p[CH_3CO\cdot]$
Termination:	$\cdot CH_3 + \cdot CH_3 \rightarrow CH_3CH_3$	$v = k_t[\cdot CH_3]^2$

The chain carriers $\cdot CH_3$ and $\cdot CHO$ are formed initially in the **initiation step**. To simplify the treatment, we shall ignore the subsequent reactions of $\cdot CHO$, except to note that they give rise to the formation of CO and of the by-product H_2. The chain carrier $\cdot CH_3$ attacks other reactant molecules in the **propagation steps**, and each attack gives rise to a new carrier. Radicals combine and end the chain in the **termination step**.

To test the proposed mechanism we need to show that it leads to the observed rate law. According to the steady-state approximation (Section 22.7b), the net rate of change of the intermediates ($\cdot CH_3$ and $CH_3CO\cdot$) may be set equal to zero:

$$\frac{d[\cdot CH_3]}{dt} = k_i[CH_3CHO] - k_p[\cdot CH_3][CH_3CHO] + k'_p[CH_3CO\cdot] - 2k_t[\cdot CH_3]^2 = 0$$

$$\frac{d[CH_3CO\cdot]}{dt} = k_p[\cdot CH_3][CH_3CHO] - k'_p[CH_3CO\cdot] = 0$$

The sum of the two equations is

$$k_i[CH_3CHO] - 2k_t[\cdot CH_3]^2 = 0$$

which shows that the steady-state approximation also implies that the rate of chain initiation is equal to the rate of chain termination. The steady-state concentration of $\cdot CH_3$ radicals is

$$[\cdot CH_3] = \left(\frac{k_i}{2k_t}\right)^{1/2} [CH_3CHO]^{1/2} \qquad (23.2)$$

It follows that the rate of formation of CH_4 is

$$\frac{d[CH_4]}{dt} = k_p[\cdot CH_3][CH_3CHO] = k_p\left(\frac{k_i}{2k_t}\right)^{1/2} [CH_3CHO]^{3/2} \qquad (23.3)$$

which is in agreement with the three-halves order observed experimentally (eqn 23.1). However, this mechanism does not accommodate the formation of various known reaction by-products, such as propanone (CH_3COCH_3) and propanal (CH_3CH_2CHO).

In many cases, a chain reaction leads to a complicated rate law. An example is the **hydrogen–bromine reaction**:

$$H_2(g) + Br_2(g) \rightarrow 2\,HBr(g) \qquad \frac{d[HBr]}{dt} = \frac{k[H_2][Br_2]^{3/2}}{[Br_2] + k'[HBr]} \qquad (23.4)$$

The following mechanism has been proposed to account for this rate law (Fig. 23.1):

Initiation: $Br_2 + M \rightarrow Br\cdot + Br\cdot + M$ $\quad v = k_i[Br_2][M]$

where M is either Br_2 or H_2. This step is an example of a **thermolysis**, a reaction initiated by heat, which stimulates vigorous intermolecular collisions.

Propagation:	$Br\cdot + H_2 \rightarrow HBr + H\cdot$	$v = k_p[Br\cdot][H_2]$
	$H\cdot + Br_2 \rightarrow HBr + Br\cdot$	$v = k'_p[H\cdot][Br_2]$
Retardation:	$H\cdot + HBr \rightarrow H_2 + Br\cdot$	$v = k_r[H\cdot][HBr]$
Termination:	$Br\cdot + Br\cdot + M \rightarrow Br_2 + M^*$	$v = k_t[Br\cdot]^2[M]$

A **retardation step** reduces the net rate of formation of product. In this case, the chain carrier H· attacks a molecule of HBr, the product. In the termination step, the third body M removes the energy of recombination. Other possible termination steps include the recombination of H atoms to form H_2 and combination of H and Br atoms. However, it turns out that only Br atom recombination is important because Br atoms propagate the chain more slowly and thus live longer than H atoms. The net rate of formation of the product HBr is

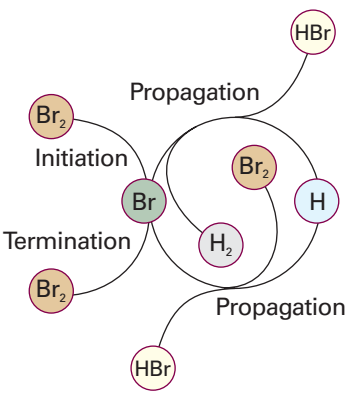

Fig. 23.1 A schematic representation of the mechanism of the reaction between hydrogen and bromine. Note how the reactants and products are shown as arms to the circle, but the intermediates (H and Br) occur only on the circle. Similar diagrams are used to depict the action of catalysts.

$$\frac{d[HBr]}{dt} = k_p[Br\cdot][H_2] + k'_p[H\cdot][Br_2] - k_r[H\cdot][HBr]$$

We can now either analyse the rate equations numerically (see *Appendix* 2 and *Further reading*) or look for approximate solutions and see if they agree with the empirical rate law. The following example illustrates the latter approach.

Example 23.1 *Deriving the rate equation of a chain reaction*

Derive the rate law for the formation of HBr according to the mechanism given above.

Method Make the steady-state approximation for the concentrations of any intermediates (H· and Br· in the present case) by setting the net rates of change of their concentrations equal to zero. Solve the resulting equations for the concentrations of the intermediates, and then use the resulting expressions in the equation for the net rate of formation of HBr.

Answer The net rates of formation of the two intermediates are

$$\frac{d[H\cdot]}{dt} = k_p[Br\cdot][H_2] - k'_p[H\cdot][Br_2] - k_r[H\cdot][HBr] = 0$$

$$\frac{d[Br\cdot]}{dt} = 2k_i[Br_2][M] - k_p[Br\cdot][H_2] + k'_p[H\cdot][Br_2] + k_r[H\cdot][HBr] - 2k_t[Br\cdot]^2[M]$$
$$= 0$$

The steady-state concentrations of the intermediates are obtained by solving these two simultaneous equations and are

$$[Br\cdot] = \left(\frac{k_i}{k_t}\right)^{1/2}[Br_2]^{1/2} \qquad [H\cdot] = \frac{k_p(k_i/k_t)^{1/2}[H_2][Br_2]^{1/2}}{k'_p[Br_2] + k_r[HBr]}$$

Note that [M] has cancelled. When we substitute these concentrations into the expression for d[HBr]/dt, we obtain

$$\frac{d[HBr]}{dt} = \frac{2k_p(k_i/k_t)^{1/2}[H_2][Br_2]^{3/2}}{[Br_2] + (k_r/k'_p)[HBr]}$$

This equation has the same form as the empirical rate law (eqn 23.4), so the two empirical rate constants can be identified as

$$k = 2k_p\left(\frac{k_i}{k_t}\right)^{1/2} \qquad k' = \frac{k_r}{k'_p}$$

The rate law shows that the reaction slows down as HBr forms, or as the [HBr]/[Br_2] ratio increases. This effect occurs because Br_2 molecules compete with HBr molecules for H· atoms, with the propagation step H· + Br_2 → HBr + Br· yielding product (HBr) and the retardation step H· + HBr → H_2 + Br· converting HBr back into reactant (H_2). Numerical integration of the rate law with mathematical software shows the predicted time dependence of the concentration of HBr for this mechanism (Fig. 23.2).

Self-test 23.1 Deduce the rate law for the production of HBr when the initiation step is the photolysis, or light-induced decomposition, of Br_2 into two bromine atoms, Br·. Let the photolysis rate be $v = I_{abs}$, where I_{abs} is the intensity of absorbed radiation. [See eqn 23.39 below]

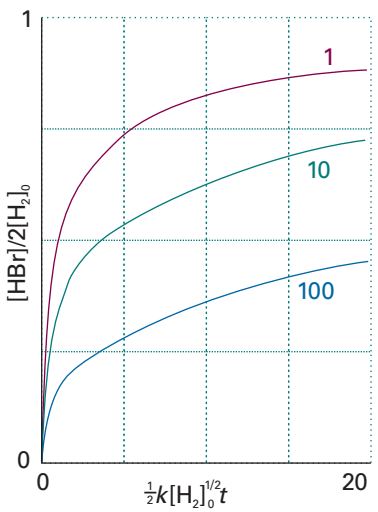

Fig. 23.2 The numerical integration of the HBr rate law, Example 23.1, can be used to explore how the concentration of HBr changes with time. These runs began with stoichiometric proportions of H_2 and Br_2; the curves are labelled with the value of $2k' - 1$.

Exploration Use mathematical software or the interactive applets found in the *Living graphs* section of the text's web site to plot the concentrations of the radicals H· and Br· against time. Find a combination of rate constants that results in steady states for these intermediates.

23.2 Explosions

A **thermal explosion** is a very rapid reaction arising from a rapid increase of reaction rate with increasing temperature. The temperature of the system rises if the energy released by an exothermic reaction cannot escape, and the reaction goes faster. The acceleration of the rate results in an even faster rise of temperature, so the reaction becomes catastrophically fast. A **chain-branching explosion** occurs when the number of chain centres grows exponentially.

An example of both types of explosion is the reaction between hydrogen and oxygen:

$$2\,H_2(g) + O_2(g) \rightarrow 2\,H_2O(g)$$

Although the net reaction is very simple, the mechanism is very complex and has not yet been fully elucidated. A chain reaction is involved, and the chain carriers include H·, ·O·, and ·OH. Some steps involving H· are:

Initiation:	$H_2 \rightarrow H\cdot + H\cdot$	$v = \text{constant}\ (v_{\text{init}})$
Propagation:	$H_2 + \cdot OH \rightarrow \cdot H + H_2O$	$v = k_p[H_2][\cdot OH]$
Branching:	$\cdot O_2\cdot + \cdot H \rightarrow \cdot O\cdot + \cdot OH$	$v = k_b[\cdot O_2\cdot][H\cdot]$
	$\cdot O\cdot + H_2 \rightarrow \cdot OH + \cdot H$	$v = k_b'[\cdot O\cdot][H_2]$
Termination:	$H\cdot + \text{wall} \rightarrow \frac{1}{2}H_2$	$v = k_t[H\cdot]$
	$H\cdot + O_2 + M \rightarrow HO_2\cdot + M^*$	$v = k_t'[H\cdot][O_2][M]$

A **branching step** is an elementary reaction that produces more than one chain carrier. Recall that an O atom, with the ground-state configuration $[He]2s^22p^4$, has two unpaired electrons. The same is true of an O_2 molecule, with 12 valence electrons and a ground-state configuration $1\sigma_g^2 1\sigma_u^2 2\sigma_g^2 1\pi_u^4 1\pi_g^2$.

The occurrence of an explosion depends on the temperature and pressure of the system, and the **explosion regions** for the reaction, the conditions under which explosion occurs, are shown in Fig. 23.3. At very low pressures the system is outside the explosion region and the mixture reacts smoothly. At these pressures the chain carriers produced in the branching steps can reach the walls of the container where they combine. Increasing the pressure along a vertical line in the illustration takes the system through the **first explosion limit** (provided the temperature is greater than about 730 K). The chain carriers react before reaching the walls and the branching reactions are explosively efficient. The reaction is smooth when the pressure is above the **second explosion limit**. The concentration of third-body M molecules is then so high compared to the concentrations of chain carriers that the combination of H· atoms with O_2 molecules to form relatively unreactive $HO_2\cdot$ molecules becomes faster than the branching reaction between H· atoms and O_2 molecules. These long-lived $HO_2\cdot$ molecules then diffuse to the walls and are removed there, in what amounts to another termination step. When the pressure is increased to above the **third explosion limit**, diffusion of $HO_2\cdot$ molecules to the walls becomes so slow that they can react with H_2 molecules (now at very high concentrations) to regenerate H atoms and H_2O_2 molecules.

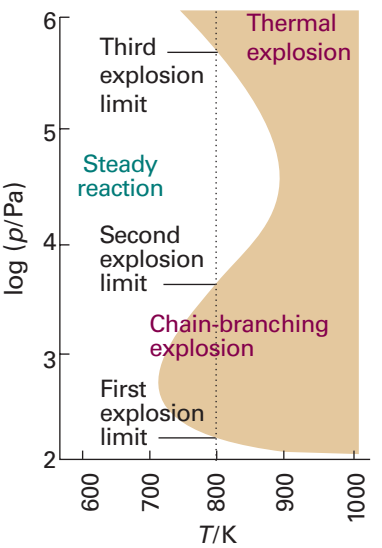

Fig. 23.3 The explosion limits of the $H_2 + O_2$ reaction. In the explosive regions the reaction proceeds explosively when heated homogeneously.

Example 23.2 *Examining the explosion behaviour of a chain reaction*

For the reaction of hydrogen and oxygen described above, show that an explosion occurs when the rate of chain branching exceeds that of chain termination.

Method Identify the onset of explosion with the rapid increase in the concentration of radicals, and for simplicity identify that concentration with the concentration of

H· atoms, which probably outnumber the highly reactive ·OH and ·O· radicals. Set up the corresponding rate laws for the reaction intermediates and then apply the steady-state approximation.

Answer The rate of formation of radicals, v_{rad}, is identified with $d[H\cdot]/dt$; therefore we write

$$v_{rad} = v_{init} + k_p[\cdot OH][H_2] - k_b[H\cdot][O_2] + k_b'[\cdot O\cdot][H_2] - k_t[H\cdot] - k_t'[H\cdot][O_2][M]$$

Applying the steady-state approximation to ·OH and ·O· gives

$$\frac{d[\cdot OH]}{dt} = -k_p[\cdot OH][H_2] + k_b[H\cdot][O_2] + k_b'[\cdot O\cdot][H_2] = 0$$

$$\frac{d[\cdot O\cdot]}{dt} = k_b[H\cdot][O_2] - k_b'[\cdot O\cdot][H_2] = 0$$

The solutions of these two algebraic equations are

$$[\cdot O\cdot] = \frac{k_b[H\cdot][O_2]}{k_b'[H_2]} \qquad [\cdot OH] = \frac{2k_b[H\cdot][O_2]}{k_p[H_2]}$$

The rate of formation of radicals is therefore

$$v_{rad} = v_{init} + (2k_b[O_2] - k_t - k_t'[O_2][M])[H\cdot]$$

We write $k_{branch} = 2k_b[O_2]$, a measure of the rate of the more important chain-branching step, and $k_{term} = k_t + k_t'[O_2][M]$, a measure of the rate of chain termination. Then,

$$\frac{d[H\cdot]}{dt} = v_{init} + (k_{branch} - k_{term})[H\cdot]$$

There are two solutions. At low O_2 concentrations, termination dominates branching, so $k_{term} > k_{branch}$. Then,

$$[H\cdot] = \frac{v_{init}}{k_{term} - k_{branch}}(1 - e^{-(k_{term}-k_{branch})t})$$

As can be seen from Fig. 23.4a, in this regime there is steady combustion of hydrogen. At high O_2 concentrations, branching dominates termination, or $k_{branch} > k_{term}$. Then,

$$[H\cdot] = \frac{v_{init}}{k_{branch} - k_{term}}(e^{(k_{branch}-k_{term})t} - 1)$$

There is now an explosive increase in the concentration of radicals (Fig. 23.4b).

Although the steady-state approximation does not hold under explosive conditions, the calculation at least gives an indication of the basis for the transition from smooth combustion to explosion.

Self-test 23.2 Calculate the variation in radical composition when the rates of branching and termination are equal. $[[H\cdot] = v_{init}t]$

Not all explosions are due to chain reactions. Solid-state explosions, such as the explosion of ammonium nitrate or TNT (2,4,6-trinitrotoluene), for instance, are simply decompositions that occur very rapidly with the production of large amounts of gas phase molecules.

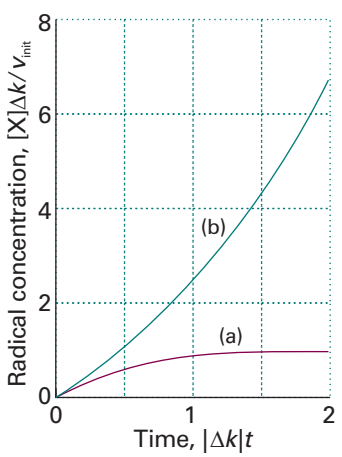

Fig. 23.4 The concentration of radicals in the fuel-rich regime of the hydrogen–oxygen reaction (a) under steady combustion conditions, (b) in the explosive region. For this graph, $\Delta k = k_{branch} - k_{term}$.

Exploration Using mathematical software, an electronic spreadsheet, or the interactive applets found in the *Living graphs* section of the text's web site, explore the effect of changing the parameter $\Delta k = k_{branch} - k_{term}$ on the shapes of the curves in Figs. 23.4a and 23.4b.

Polymerization kinetics

In **stepwise polymerization** any two monomers present in the reaction mixture can link together at any time and growth of the polymer is not confined to chains that are already forming (Fig. 23.5). As a result, monomers are removed early in the reaction and, as we shall see, the average molar mass of the product grows with time. In **chain polymerization** an activated monomer, M, attacks another monomer, links to it, then that unit attacks another monomer, and so on. The monomer is used up as it becomes linked to the growing chains (Fig. 23.6). High polymers are formed rapidly and only the yield, not the average molar mass, of the polymer is increased by allowing long reaction times.

23.3 Stepwise polymerization

Stepwise polymerization commonly proceeds by a condensation reaction, in which a small molecule (typically H_2O) is eliminated in each step. Stepwise polymerization is the mechanism of production of polyamides, as in the formation of nylon-66:

$$\begin{aligned} &H_2N(CH_2)_6NH_2 + HOOC(CH_2)_4COOH \\ &\quad \rightarrow H_2N(CH_2)_6NHCO(CH_2)_4COOH + H_2O \\ &\quad \rightarrow H{-}[NH(CH_2)_6NHCO(CH_2)_4CO]_n{-}OH \end{aligned}$$

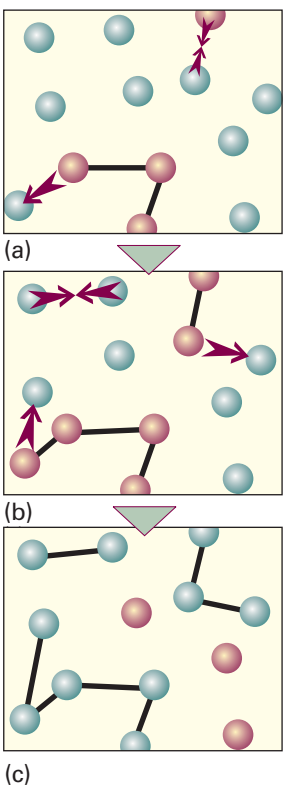

Fig. 23.5 In stepwise polymerization, growth can start at any pair of monomers, and so new chains begin to form throughout the reaction.

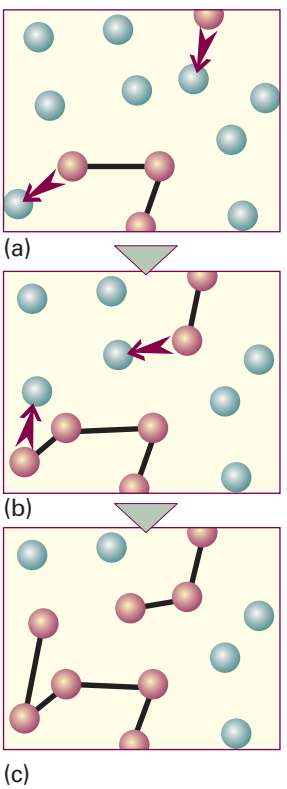

Fig. 23.6 The process of chain polymerization. Chains grow as each chain acquires additional monomers.

Polyesters and polyurethanes are formed similarly (the latter without elimination). A polyester, for example, can be regarded as the outcome of the stepwise condensation of a hydroxyacid HO—M—COOH. We shall consider the formation of a polyester from such a monomer, and measure its progress in terms of the concentration of the —COOH groups in the sample (which we denote A), for these groups gradually disappear as the condensation proceeds. Because the condensation reaction can occur between molecules containing any number of monomer units, chains of many different lengths can grow in the reaction mixture.

In the absence of a catalyst, we can expect the condensation to be overall second-order in the concentration of the —OH and —COOH (or A) groups, and write

$$\frac{d[A]}{dt} = -k[OH][A] \tag{23.5a}$$

However, because there is one —OH group for each —COOH group, this equation is the same as

$$\frac{d[A]}{dt} = -k[A]^2 \tag{23.5b}$$

If we assume that the rate constant for the condensation is independent of the chain length, then k remains constant throughout the reaction. The solution of this rate law is given by eqn 22.15, and is

$$[A] = \frac{[A]_0}{1 + kt[A]_0} \tag{23.6}$$

The fraction, p, of —COOH groups that have condensed at time t is, after application of eqn 23.6:

$$p = \frac{[A]_0 - [A]}{[A]_0} = \frac{kt[A]_0}{1 + kt[A]_0} \tag{23.7}$$

Next, we calculate the **degree of polymerization**, which is defined as the average number of monomer residues per polymer molecule. This quantity is the ratio of the initial concentration of A, $[A]_0$, to the concentration of end groups, [A], at the time of interest, because there is one —A group per polymer molecule. For example, if there were initially 1000 A groups and there are now only 10, each polymer must be 100 units long on average. Because we can express [A] in terms of p (eqn 23.7), the average number of monomers per polymer molecule, $<n>$, is

$$<n> = \frac{[A]_0}{[A]} = \frac{1}{1 - p} \tag{23.8a}$$

This result is illustrated in Fig. 23.7. When we express p in terms of the rate constant k (eqn 23.7), we find

$$<n> = 1 + kt[A]_0 \tag{23.8b}$$

The average length grows linearly with time. Therefore, the longer a stepwise polymerization proceeds, the higher the average molar mass of the product.

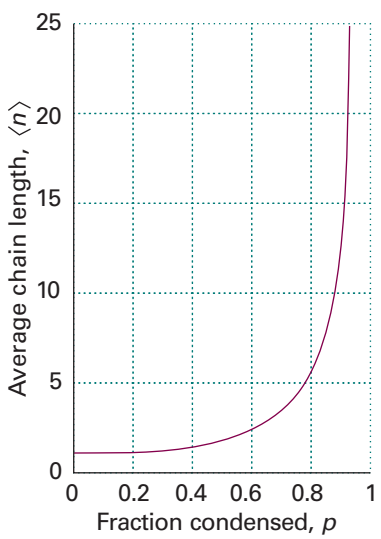

Fig. 23.7 The average chain length of a polymer as a function of the fraction of reacted monomers, p. Note that p must be very close to 1 for the chains to be long.

Exploration Plot the variation of p with time for a range of k values of your choosing (take $[A]_0 = 1.0$ mol dm^{-3}).

23.4 Chain polymerization

Chain polymerization occurs by addition of monomers to a growing polymer, often by a radical chain process. It results in the rapid growth of an individual polymer

chain for each activated monomer. Examples include the addition polymerizations of ethene, methyl methacrylate, and styrene, as in

$$-CH_2CHX\cdot + CH_2{=}CHX \rightarrow -CH_2CHXCH_2CHX\cdot$$

and subsequent reactions. The central feature of the kinetic analysis (which is summarized in the *Justification* below) is that the rate of polymerization is proportional to the square root of the initiator concentration:

$$v = k[\mathrm{I}]^{1/2}[\mathrm{M}] \tag{23.9}$$

Justification 23.1 *The rate of chain polymerization*

There are three basic types of reaction step in a chain polymerization process:

(a) Initiation:

$$\mathrm{I} \rightarrow \mathrm{R}\cdot + \mathrm{R}\cdot \qquad v_\mathrm{i} = k_\mathrm{i}[\mathrm{I}]$$
$$\mathrm{M} + \mathrm{R}\cdot \rightarrow \cdot\mathrm{M}_1 \qquad \text{(fast)}$$

where I is the initiator, R· the radical I forms, and $\cdot M_1$ is a monomer radical. We have shown a reaction in which a radical is produced, but in some polymerizations the initiation step leads to the formation of an ionic chain carrier. The rate-determining step is the formation of the radicals R· by homolysis of the initiator, so the rate of initiation is equal to the v_i given above.

(b) Propagation:

$$\mathrm{M} + \cdot\mathrm{M}_1 \rightarrow \cdot\mathrm{M}_2$$
$$\mathrm{M} + \cdot\mathrm{M}_2 \rightarrow \cdot\mathrm{M}_3$$
$$\vdots$$
$$\mathrm{M} + \cdot\mathrm{M}_{n-1} \rightarrow \cdot\mathrm{M}_n \qquad v_\mathrm{p} = k_\mathrm{p}[\mathrm{M}][\cdot\mathrm{M}]$$

If we assume that the rate of propagation is independent of chain size for sufficiently large chains, then we can use only the equation given above to describe the propagation process. Consequently, for sufficiently large chains, the rate of propagation is equal to the overall rate of polymerization.

Because this chain of reactions propagates quickly, the rate at which the total concentration of radicals grows is equal to the rate of the rate-determining initiation step. It follows that

$$\left(\frac{\mathrm{d}[\cdot\mathrm{M}]}{\mathrm{d}t}\right)_{\text{production}} = 2fk_\mathrm{i}[\mathrm{I}] \tag{23.10}$$

where f is the fraction of radicals R· that successfully initiate a chain.

(c) Termination:

$$\cdot\mathrm{M}_n + \cdot\mathrm{M}_m \rightarrow \mathrm{M}_{n+m} \qquad \text{(mutual termination)}$$
$$\cdot\mathrm{M}_n + \cdot\mathrm{M}_m \rightarrow \mathrm{M}_n + \mathrm{M}_m \qquad \text{(disproportionation)}$$
$$\mathrm{M} + \cdot\mathrm{M}_n \rightarrow \cdot\mathrm{M} + \mathrm{M}_n \qquad \text{(chain transfer)}$$

In **mutual termination** two growing radical chains combine. In termination by **disproportionation** a hydrogen atom transfers from one chain to another, corresponding to the oxidation of the donor and the reduction of the acceptor. In **chain transfer**, a new chain initiates at the expense of the one currently growing.

Here we suppose that only mutual termination occurs. If we assume that the rate of termination is independent of the length of the chain, the rate law for termination is

$$v_\mathrm{t} = k_\mathrm{t}[\cdot\mathrm{M}]^2$$

and the rate of change of radical concentration by this process is

$$\left(\frac{\mathrm{d}[\cdot\mathrm{M}]}{\mathrm{d}t}\right)_{\text{depletion}} = -2k_t[\cdot\mathrm{M}]^2$$

The steady-state approximation gives:

$$\frac{\mathrm{d}[\cdot\mathrm{M}]}{\mathrm{d}t} = 2fk_i[\mathrm{I}] - 2k_t[\cdot\mathrm{M}]^2 = 0$$

The steady-state concentration of radical chains is therefore

$$[\cdot\mathrm{M}] = \left(\frac{fk_i}{k_t}\right)^{1/2}[\mathrm{I}]^{1/2} \tag{23.11}$$

Because the rate of propagation of the chains is the negative of the rate at which the monomer is consumed, we can write $v_P = -\mathrm{d}[\mathrm{M}]/\mathrm{d}t$ and

$$v_P = k_P[\cdot\mathrm{M}][\mathrm{M}] = k_P\left(\frac{fk_i}{k_t}\right)^{1/2}[\mathrm{I}]^{1/2}[\mathrm{M}] \tag{23.12}$$

This rate is also the rate of polymerization, which has the form of eqn 23.9.

The **kinetic chain length**, ν, is the ratio of the number of monomer units consumed per activated centre produced in the initiation step:

$$\nu = \frac{\text{number of monomer units consumed}}{\text{number of activated centres produced}} \tag{23.13}$$

The kinetic chain length can be expressed in terms of the rate expressions in *Justification* 23.1. To do so, we recognize that monomers are consumed at the rate that chains propagate. Then,

$$\nu = \frac{\text{rate of propagation of chains}}{\text{rate of production of radicals}}$$

By making the steady-state approximation, we set the rate of production of radicals equal to the termination rate. Therefore, we can write the expression for the kinetic chain length as

$$\nu = \frac{k_P[\cdot\mathrm{M}][\mathrm{M}]}{2k_t[\mathrm{M}\cdot]^2} = \frac{k_P[\mathrm{M}]}{2k_t[\cdot\mathrm{M}]}$$

When we substitute the steady-state expression, eqn 23.11, for the radical concentration, we obtain

$$\nu = k[\mathrm{M}][\mathrm{I}]^{-1/2} \qquad k = \tfrac{1}{2}k_P(fk_ik_t)^{-1/2} \tag{23.14}$$

Consider a polymer produced by a chain mechanism with mutual termination. In this case, the average number of monomers in a polymer molecule, $<n>$, produced by the reaction is the sum of the numbers in the two combining polymer chains. The average number of units in each chain is ν. Therefore,

$$<n> = 2\nu = 2k[\mathrm{M}][\mathrm{I}]^{-1/2} \tag{23.15}$$

with k given in eqn 23.14. We see that, the slower the initiation of the chain (the smaller the initiator concentration and the smaller the initiation rate constant), the greater the kinetic chain length, and therefore the higher the average molar mass of the polymer. Some of the consequences of molar mass for polymers were explored in Chapter 19: now we have seen how we can exercise kinetic control over them.

Homogeneous catalysis

A **catalyst** is a substance that accelerates a reaction but undergoes no net chemical change. The catalyst lowers the activation energy of the reaction by providing an alternative path that avoids the slow, rate-determining step of the uncatalysed reaction (Fig. 23.8). Catalysts can be very effective; for instance, the activation energy for the decomposition of hydrogen peroxide in solution is 76 kJ mol^{-1}, and the reaction is slow at room temperature. When a little iodide ion is added, the activation energy falls to 57 kJ mol^{-1} and the rate constant increases by a factor of 2000. **Enzymes**, which are biological catalysts, are very specific and can have a dramatic effect on the reactions they control. For example, the enzyme catalase reduces the activation energy for the decomposition of hydrogen peroxide to 8 kJ mol^{-1}, corresponding to an acceleration of the reaction by a factor of 10^{15} at 298 K.

A **homogeneous catalyst** is a catalyst in the same phase as the reaction mixture. For example, the decomposition of hydrogen peroxide in aqueous solution is catalysed by bromide ion or catalase (Sections 23.5 and 23.6). A **heterogeneous catalyst** is a catalyst in a different phase from the reaction mixture. For example, the hydrogenation of ethene to ethane, a gas-phase reaction, is accelerated in the presence of a solid catalyst such as palladium, platinum, or nickel. The metal provides a surface upon which the reactants bind; this binding facilitates encounters between reactants and increases the rate of the reaction. We examine heterogeneous catalysis in Chapter 25 and consider only homogeneous catalysis here.

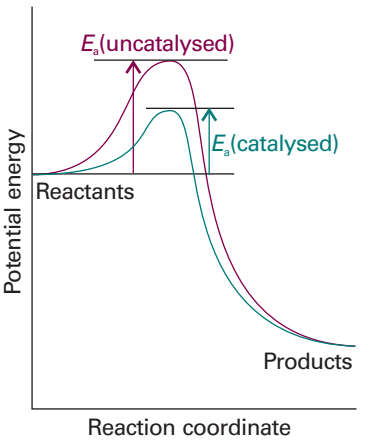

Fig. 23.8 A catalyst provides a different path with a lower activation energy. The result is an increase in the rate of formation of products.

23.5 Features of homogeneous catalysis

We can obtain some idea of the mode of action of homogeneous catalysts by examining the kinetics of the bromide-catalysed decomposition of hydrogen peroxide:

$$2\,H_2O_2(aq) \rightarrow 2\,H_2O(l) + O_2(g)$$

The reaction is believed to proceed through the following pre-equilibrium:

$$H_3O^+ + H_2O_2 \rightleftharpoons H_3O_2^+ + H_2O \qquad K = \frac{[H_3O_2^+]}{[H_2O_2][H_3O^+]}$$

$$H_3O_2^+ + Br^- \rightarrow HOBr + H_2O \qquad v = k[H_3O_2^+][Br^-]$$

$$HOBr + H_2O_2 \rightarrow H_3O^+ + O_2 + Br^- \qquad \text{(fast)}$$

where we have set the activity of H_2O in the equilibrium constant equal to 1 and assumed that the thermodynamic properties of the other substances are ideal. The second step is rate-determining. Therefore, we can obtain the rate law of the overall reaction by setting the overall rate equal to the rate of the second step and using the equilibrium constant to express the concentration of $H_3O_2^+$ in terms of the reactants. The result is

$$\frac{d[O_2]}{dt} = k_{eff}[H_2O_2][H_3O^+][Br^-]$$

with $k_{eff} = kK$, in agreement with the observed dependence of the rate on the Br^- concentration and the pH of the solution. The observed activation energy is that of the effective rate constant kK.

In **acid catalysis** the crucial step is the transfer of a proton to the substrate:

$$X + HA \rightarrow HX^+ + A^- \qquad HX^+ \rightarrow \text{products}$$

Acid catalysis is the primary process in the solvolysis of esters and keto–enol tautomerism. In **base catalysis**, a proton is transferred from the substrate to a base:

$$XH + B \rightarrow X^- + BH^+ \qquad X^- \rightarrow \text{products}$$

Base catalysis is the primary step in the isomerization and halogenation of organic compounds, and of the Claisen and aldol condensation reactions.

23.6 Enzymes

Enzymes are homogeneous biological catalysts. These ubiquitous compounds are special proteins or nucleic acids that contain an **active site**, which is responsible for binding the **substrates**, the reactants, and processing them into products. As is true of any catalyst, the active site returns to its original state after the products are released. Many enzymes consist primarily of proteins, some featuring organic or inorganic co-factors in their active sites. However, certain RNA molecules can also be biological catalysts, forming **ribozymes**. A very important example of a ribozyme is the **ribosome**, a large assembly of proteins and catalytically active RNA molecules responsible for the synthesis of proteins in the cell.

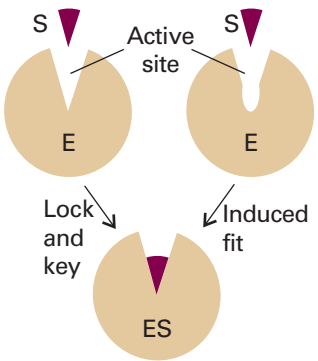

Fig. 23.9 Two models that explain the binding of a substrate to the active site of an enzyme. In the lock-and-key model, the active site and substrate have complementary three-dimensional structures and dock perfectly without the need for major atomic rearrangements. In the induced fit model, binding of the substrate induces a conformational change in the active site. The substrate fits well in the active site after the conformational change has taken place.

The structure of the active site is specific to the reaction that it catalyses, with groups in the substrate interacting with groups in the active site by intermolecular interactions, such as hydrogen bonding, electrostatic, or van der Waals interactions. Figure 23.9 shows two models that explain the binding of a substrate to the active site of an enzyme. In the **lock-and-key model**, the active site and substrate have complementary three-dimensional structures and dock perfectly without the need for major atomic rearrangements. Experimental evidence favours the **induced fit model**, in which binding of the substrate induces a conformational change in the active site. Only after the change does the substrate fit snugly in the active site.

Enzyme-catalysed reactions are prone to inhibition by molecules that interfere with the formation of product. Many drugs for the treatment of disease function by inhibiting enzymes. For example, an important strategy in the treatment of acquired immune deficiency syndrome (AIDS) involves the steady administration of a specially designed protease inhibitor. The drug inhibits an enzyme that is key to the formation of the protein envelope surrounding the genetic material of the human immunodeficiency virus (HIV). Without a properly formed envelope, HIV cannot replicate in the host organism.

(a) The Michaelis–Menten mechanism of enzyme catalysis

Experimental studies of enzyme kinetics are typically conducted by monitoring the initial rate of product formation in a solution in which the enzyme is present at very low concentration. Indeed, enzymes are such efficient catalysts that significant accelerations may be observed even when their concentration is more than three orders of magnitude smaller than that of the substrate.

The principal features of many enzyme-catalysed reactions are as follows:

1 For a given initial concentration of substrate, $[S]_0$, the initial rate of product formation is proportional to the total concentration of enzyme, $[E]_0$.

2 For a given $[E]_0$ and low values of $[S]_0$, the rate of product formation is proportional to $[S]_0$.

3 For a given $[E]_0$ and high values of $[S]_0$, the rate of product formation becomes independent of $[S]_0$, reaching a maximum value known as the **maximum velocity**, v_{max}.

The **Michaelis–Menten mechanism** accounts for these features. According to this mechanism, an enzyme–substrate complex is formed in the first step and either the substrate is released unchanged or after modification to form products:

$$\begin{aligned} &E + S \rightleftharpoons ES && k_a, k'_a \\ &ES \rightarrow P && k_b \end{aligned} \tag{23.16}$$

We show in the following *Justification* that this mechanism leads to the **Michaelis–Menten equation** for the rate of product formation

$$v = \frac{k_b[E]_0}{1 + K_m/[S]_0} \tag{23.17}$$

where $K_M = (k'_a + k_b)/k_a$ is the **Michaelis constant**, characteristic of a given enzyme acting on a given substrate.

Justification 23.2 *The Michaelis–Menten equation*

The rate of product formation according to the Michaelis–Menten mechanism is

$$v = k_b[ES] \tag{23.18}$$

We can obtain the concentration of the enzyme–substrate complex by invoking the steady-state approximation and writing

$$\frac{d[ES]}{dt} = k_a[E][S] - k'_a[ES] - k_b[ES] = 0$$

It follows that

$$[ES] = \left(\frac{k_a}{k'_a + k_b}\right)[E][S] \tag{23.19}$$

where [E] and [S] are the concentrations of *free* enzyme and substrate, respectively. Now we define the Michaelis constant as

$$K_M = \frac{k'_a + k_b}{k_a} = \frac{[E][S]}{[ES]}$$

and note that K_M has the same units as molar concentration. To express the rate law in terms of the concentrations of enzyme and substrate added, we note that $[E]_0 = [E] + [ES]$. Moreover, because the substrate is typically in large excess relative to the enzyme, the free substrate concentration is approximately equal to the initial substrate concentration and we can write $[S] \approx [S]_0$. It then follows that:

$$[ES] = \frac{[E]_0}{1 + K_M/[S]_0}$$

We obtain eqn 23.17 when we substitute this expression for [ES] into that for the rate of product formation ($v = k_b[ES]$).

Equation 23.17 shows that, in accord with experimental observations (Fig. 23.10):

1 When $[S]_0 \ll K_M$, the rate is proportional to $[S]_0$:

$$v = \frac{k_a}{K_M}[S]_0[E]_0 \tag{23.20a}$$

2 When $[S]_0 \gg K_M$, the rate reaches its maximum value and is independent of $[S]_0$:

$$v = v_{max} = k_b[E]_0 \tag{23.20b}$$

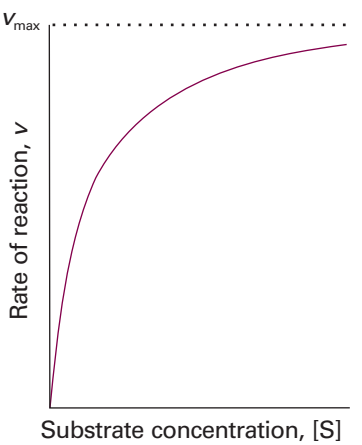

Fig. 23.10 The variation of the rate of an enzyme-catalysed reaction with substrate concentration. The approach to a maximum rate, v_{max}, for large [S] is explained by the Michaelis–Menten mechanism.

Exploration Use the Michaelis–Menten equation to generate two families of curves showing the dependence of v on [S]: one in which K_M varies but v_{max} is constant, and another in which v_{max} varies but K_M is constant.

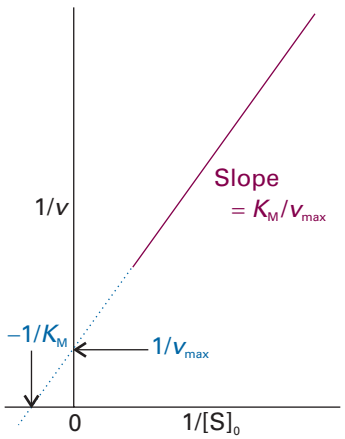

Fig. 23.11 A Lineweaver–Burk plot for the analysis of an enzyme-catalysed reaction that proceeds by a Michaelis–Menten mechanism and the significance of the intercepts and the slope.

Substitution of the definitions of K_M and v_{max} into eqn 23.17 gives:

$$v = \frac{v_{max}}{1 + K_M/[S]_0} \tag{23.21}$$

We can rearrange this expression into a form that is amenable to data analysis by linear regression:

$$\frac{1}{v} = \frac{1}{v_{max}} + \left(\frac{K_M}{v_{max}}\right)\frac{1}{[S]_0} \tag{23.22}$$

A **Lineweaver–Burk plot** is a plot of $1/v$ against $1/[S]_0$, and according to eqn 23.22 it should yield a straight line with slope of K_M/v_{max}, a y-intercept at $1/v_{max}$, and an x-intercept at $-1/K_M$ (Fig. 23.11). The value of k_b is then calculated from the y-intercept and eqn 23.20b. However, the plot cannot give the individual rate constants k_a and k'_a that appear in the expression for K_M. The stopped-flow technique described in Section 22.1b can give the additional data needed, because we can find the rate of formation of the enzyme–substrate complex by monitoring the concentration after mixing the enzyme and substrate. This procedure gives a value for k_a, and k'_a is then found by combining this results with the values of k_b and K_M.

(b) The catalytic efficiency of enzymes

The **turnover frequency**, or **catalytic constant**, of an enzyme, k_{cat}, is the number of catalytic cycles (turnovers) performed by the active site in a given interval divided by the duration of the interval. This quantity has units of a first-order rate constant and, in terms of the Michaelis–Menten mechanism, is numerically equivalent to k_b, the rate constant for release of product from the enzyme–substrate complex. It follows from the identification of k_{cat} with k_b and from eqn 23.20b that

$$k_{cat} = k_b = \frac{v_{max}}{[E]_0} \tag{23.23}$$

The **catalytic efficiency**, ε (epsilon), of an enzyme is the ratio k_{cat}/K_M. The higher the value of ε, the more efficient is the enzyme. We can think of the catalytic activity as the effective rate constant of the enzymatic reaction. From $K_M = (k'_a + k_b)/k_a$ and eqn 23.23, it follows that

$$\varepsilon = \frac{k_{cat}}{K_m} = \frac{k_a k_b}{k'_a + k_b} \tag{23.24}$$

The efficiency reaches its maximum value of k_a when $k_b \gg k'_a$. Because k_a is the rate constant for the formation of a complex from two species that are diffusing freely in solution, the maximum efficiency is related to the maximum rate of diffusion of E and S in solution. This limit (which is discussed further in Section 24.2) leads to rate constants of about 10^8–10^9 dm^3 mol^{-1} s^{-1} for molecules as large as enzymes at room temperature. The enzyme catalase has $\varepsilon = 4.0 \times 10^8$ dm^3 mol^{-1} s^{-1} and is said to have attained 'catalytic perfection', in the sense that the rate of the reaction it catalyses is controlled only by diffusion: it acts as soon as a substrate makes contact.

Comment 23.1
The web site contains links to databases of enzymes.

Example 23.3 *Determining the catalytic efficiency of an enzyme*

The enzyme carbonic anhydrase catalyses the hydration of CO_2 in red blood cells to give bicarbonate (hydrogencarbonate) ion:

$$CO_2(g) + H_2O(l) \rightarrow HCO_3^-(aq) + H^+(aq)$$

The following data were obtained for the reaction at pH = 7.1, 273.5 K, and an enzyme concentration of 2.3 nmol dm^{-3}:

$[CO_2]$/(mmol dm^{-3})	1.25	2.5	5	20
rate/(mmol dm^{-3} s^{-1})	2.78×10^{-2}	5.00×10^{-2}	8.33×10^{-2}	1.67×10^{-1}

Determine the catalytic efficiency of carbonic anhydrase at 273.5 K.

Method Prepare a Lineweaver–Burk plot and determine the values of K_M and v_{max} by linear regression analysis. From eqn 23.23 and the enzyme concentration, calculate k_{cat} and the catalytic efficiency from eqn 23.24.

Answer We draw up the following table:

$1/([CO_2]/(\text{mmol dm}^{-3}))$	0.800	0.400	0.200	0.0500
$1/(v/(\text{mmol dm}^{-3}\ \text{s}^{-1}))$	36.0	20.0	12.0	6.0

Figure 23.12 shows the Lineweaver–Burk plot for the data. The slope is 40.0 and the y-intercept is 4.00. Hence,

$$v_{max}/(\text{mmol dm}^{-3}\ \text{s}^{-1}) = \frac{1}{\text{intercept}} = \frac{1}{4.00} = 0.250$$

and

$$K_M/(\text{mmol dm}^{-3}) = \frac{\text{slope}}{\text{intercept}} = \frac{40.0}{4.00} = 10.0$$

It follows that

$$k_{cat} = \frac{v_{max}}{[E]_0} = \frac{2.5 \times 10^{-4}\ \text{mol dm}^{-3}\ \text{s}^{-1}}{2.3 \times 10^{-9}\ \text{mol dm}^{-3}} = 1.1 \times 10^5\ \text{s}^{-1}$$

and

$$\varepsilon = \frac{k_{cat}}{K_M} = \frac{1.1 \times 10^5\ \text{s}^{-1}}{1.0 \times 10^{-2}\ \text{mol dm}^{-3}} = 1.1 \times 10^7\ \text{dm}^3\ \text{mol}^{-1}\ \text{s}^{-1}$$

A note on good practice The slope and the intercept are unit-less: we have remarked previously, that all graphs should be plotted as pure numbers.

Self-test 23.3 The enzyme α-chymotrypsin is secreted in the pancreas of mammals and cleaves peptide bonds made between certain amino acids. Several solutions containing the small peptide *N*-glutaryl-L-phenylalanine-*p*-nitroanilide at different concentrations were prepared and the same small amount of α-chymotrypsin was added to each one. The following data were obtained on the initial rates of the formation of product:

[S]/(mmol dm^{-3})	0.334	0.450	0.667	1.00	1.33	1.67
v/(mmol dm^{-3} s^{-1})	0.152	0.201	0.269	0.417	0.505	0.667

Determine the maximum velocity and the Michaelis constant for the reaction.

[$v_{max} = 2.80$ mmol dm^{-3} s^{-1}, $K_M = 5.89$ mmol dm^{-3}]

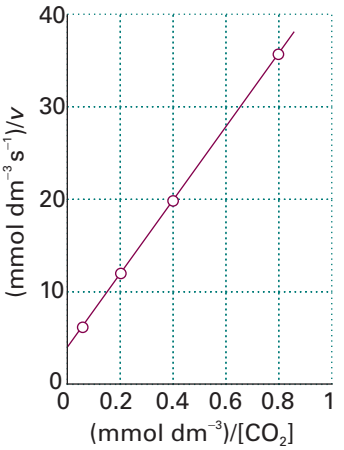

Fig. 23.12 The Lineweaver–Burk plot of the data for Example 23.3.

(c) Mechanisms of enzyme inhibition

An inhibitor, I, decreases the rate of product formation from the substrate by binding to the enzyme, to the ES complex, or to the enzyme and ES complex simultaneously. The most general kinetic scheme for enzyme inhibition is then:

$$\mathrm{E + S \rightleftharpoons ES} \qquad k_a, k'_a$$

$$\mathrm{ES \rightarrow E + P} \qquad k_b$$

$$\mathrm{EI \rightleftharpoons E + I} \qquad K_I = \frac{[E][I]}{[EI]} \tag{23.25a}$$

$$\mathrm{ESI \rightleftharpoons ES + I} \qquad K'_S = \frac{[E][I]}{[EI]} \tag{23.25b}$$

The lower the values of K_I and K'_I the more efficient are the inhibitors. The rate of product formation is always given by $v = k_b[ES]$, because only ES leads to product. As shown in the following *Justification*, the rate of reaction in the presence of an inhibitor is

$$v = \frac{v_{max}}{\alpha' + \alpha K_M/[S]_0} \tag{23.26}$$

where $\alpha = 1 + [I]/K_I$ and $\alpha' = 1 + [I]/K'_I$. This equation is very similar to the Michaelis–Menten equation for the uninhibited enzyme (eqn 23.17) and is also amenable to analysis by a Lineweaver–Burk plot:

$$\frac{1}{v} = \frac{\alpha'}{v_{max}} + \left(\frac{\alpha K_M}{v_{max}}\right)\frac{1}{[S]_0} \tag{23.27}$$

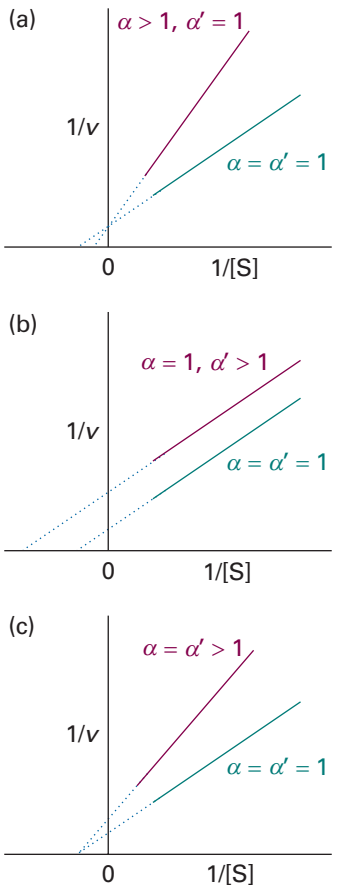

Fig. 23.13 Lineweaver–Burk plots characteristic of the three major modes of enzyme inhibition: (a) competitive inhibition, (b) uncompetitive inhibition, and (c) non-competitive inhibition, showing the special case $\alpha = \alpha' > 1$.

Exploration Use eqn 23.26 to explore the effect of competitive, uncompetitive, and non-competitive inhibition on the shapes of the plots of v against [S] for constant K_M and v_{max}.

Justification 23.3 *Enzyme inhibition*

By mass balance, the total concentration of enzyme is:

$$[E]_0 = [E] + [EI] + [ES] + [ESI]$$

By using eqns 23.25a and 23.25b and the definitions

$$\alpha = 1 + \frac{[I]}{K_I} \qquad \text{and} \qquad \alpha' = 1 + \frac{[I]}{K'_I}$$

it follows that

$$[E]_0 = [E]\alpha + [ES]\alpha'$$

By using $K_M = [E][S]/[ES]$, we can write

$$[E]_0 = \frac{K_M[ES]}{[S]_0}\alpha + [ES]\alpha' = [ES]\left(\frac{\alpha K_M}{[S]_0} + \alpha'\right)$$

The expression for the rate of product formation is then:

$$v = k_b[ES] = \frac{k_b[E]_0}{\alpha K_M/[S]_0 + \alpha'}$$

which, upon rearrangement, gives eqn 23.26.

There are three major modes of inhibition that give rise to distinctly different kinetic behaviour (Fig. 23.13). In **competitive inhibition** the inhibitor binds only to the active site of the enzyme and thereby inhibits the attachment of the substrate. This condition corresponds to $\alpha > 1$ and $\alpha' = 1$ (because ESI does not form). The slope of

the Lineweaver–Burk plot increases by a factor of α relative to the slope for data on the uninhibited enzyme ($\alpha = \alpha' = 1$). The y-intercept does not change as a result of competitive inhibition (Fig. 23.13a). In **uncompetitive inhibition** the inhibitor binds to a site of the enzyme that is removed from the active site, but only if the substrate is already present. The inhibition occurs because ESI reduces the concentration of ES, the active type of complex. In this case $\alpha = 1$ (because EI does not form) and $\alpha' > 1$. The y-intercept of the Lineweaver–Burk plot increases by a factor of α' relative to the y-intercept for data on the uninhibited enzyme but the slope does not change (Fig. 23.13b). In **non-competitive inhibition** (also called **mixed inhibition**) the inhibitor binds to a site other than the active site, and its presence reduces the ability of the substrate to bind to the active site. Inhibition occurs at both the E and ES sites. This condition corresponds to $\alpha > 1$ and $\alpha' > 1$. Both the slope and y-intercept of the Lineweaver–Burk plot increase upon addition of the inhibitor. Figure 23.13c shows the special case of $K_I = K_I'$ and $\alpha = \alpha'$, which results in intersection of the lines at the x-axis.

In all cases, the efficiency of the inhibitor may be obtained by determining K_M and v_{max} from a control experiment with uninhibited enzyme and then repeating the experiment with a known concentration of inhibitor. From the slope and y-intercept of the Lineweaver–Burk plot for the inhibited enzyme (eqn 23.27), the mode of inhibition, the values of α or α', and the values of K_I or K_I' may be obtained.

Photochemistry

Many reactions can be initiated by the absorption of electromagnetic radiation by one of the mechanisms described in Chapter 14. The most important of all are the photochemical processes that capture the radiant energy of the Sun. Some of these reactions lead to the heating of the atmosphere during the daytime by absorption of ultraviolet radiation (*Impact* I23.1). Others include the absorption of visible radiation during photosynthesis (*Impact* I7.2 and I23.2). Without photochemical processes, the Earth would be simply a warm, sterile, rock. Table 23.1 summarizes common photochemical reactions.

23.7 Kinetics of photophysical and photochemical processes

Photochemical processes are initiated by the absorption of radiation by at least one component of a reaction mixture. In a **primary process**, products are formed directly from the excited state of a reactant. Examples include fluorescence (Section 14.3) and the *cis–trans* photoisomerization of retinal (Table 23.1, see also *Impact* I14.1). Products of a **secondary process** originate from intermediates that are formed directly from the excited state of a reactant. Examples include photosynthesis and photochemical chain reactions (Section 23.8).

Competing with the formation of photochemical products is a host of primary photophysical processes that can deactivate the excited state (Table 23.2). Therefore, it is important to consider the timescales of excited state formation and decay before describing the mechanisms of photochemical reactions.

Comment 23.2
The web site contains links to databases on photochemical reactions.

(a) Timescales of photophysical processes

Electronic transitions caused by absorption of ultraviolet and visible radiation occur within 10^{-16}–10^{-15} s. We expect, then, that the upper limit for the rate constant of a first-order photochemical reaction is about 10^{16} s^{-1}. Fluorescence is slower than

Table 23.1 Examples of photochemical processes

Process	General form	Example
Ionization	$A^* \rightarrow A^+ + e^-$	$NO^* \xrightarrow{134\ nm} NO^+ + e^-$
Electron transfer	$A^* + B \rightarrow A^+ + B^-$ or $A^- + B^+$	$[Ru(bpy)_3^{2+}]^* + Fe^{3+} \xrightarrow{452\ nm} Ru(bpy)_3^{3+} + Fe^{2+}$
Dissociation	$A^* \rightarrow B + C$	$O_3^* \xrightarrow{1180\ nm} O_2 + O$
	$A^* + B{-}C \rightarrow A + B + C$	$Hg^* + CH_4 \xrightarrow{254\ nm} Hg + CH_3 + H$
Addition	$2\ A^* \rightarrow B$	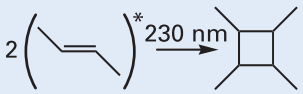
	$A^* + B \rightarrow AB$	
Abstraction	$A^* + B{-}C \rightarrow A{-}B + C$	$Hg^* + H_2 \xrightarrow{254\ nm} HgH + H$
Isomerization or rearrangement	$A^* \rightarrow A'$	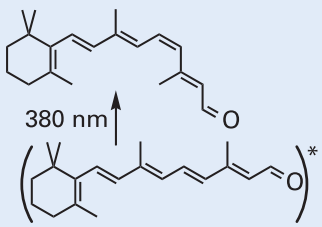

* Excited state.

Table 23.2 Common photophysical processes†

Primary absorption	$S + h\nu \rightarrow S^*$
Excited-state absorption	$S^* + h\nu \rightarrow S^{**}$
	$T^* + h\nu \rightarrow T^{**}$
Fluorescence	$S^* \rightarrow S + h\nu$
Stimulated emission	$S^* + h\nu \rightarrow S + 2h\nu$
Intersystem crossing (ISC)	$S^* \rightarrow T^*$
Phosphorescence	$T^* \rightarrow S + h\nu$
Internal conversion (IC)	$S^* \rightarrow S$
Collision-induced emission	$S^* + M \rightarrow S + M + h\nu$
Collisional deactivation	$S^* + M \rightarrow S + M$
	$T^* + M \rightarrow S + M$
Electronic energy transfer:	
Singlet–singlet	$S^* + S \rightarrow S + S^*$
Triple–triplet	$T^* + T \rightarrow T + T^*$
Excimer formation	$S^* + S \rightarrow (SS)^*$
Energy pooling	
Singlet–singlet	$S^* + S^* \rightarrow S^{**} + S$
Triple–triplet	$T^* + T^* \rightarrow S^* + S$

† S denotes a singlet state, T a triplet state, and M is a third body.

absorption, with typical lifetimes of 10^{-12}–10^{-6} s. Therefore, the excited singlet state can initiate very fast photochemical reactions in the femtosecond (10^{-15} s) to picosecond (10^{-12} s) timescale. Examples of such ultrafast reactions are the initial events of vision (*Impact* I14.1) and of photosynthesis. Typical intersystem crossing (ISC) and phosphorescence times for large organic molecules are 10^{-12}–10^{-4} s and 10^{-6}–10^{-1} s, respectively. As a consequence, excited triplet states are photochemically important. Indeed, because phosphorescence decay is several orders of magnitude slower than most typical reactions, species in excited triplet states can undergo a very large number of collisions with other reactants before deactivation. The interplay between reaction rates and excited state lifetimes is a very important factor in the determination of the kinetic feasibility of a photochemical process.

Illustration 23.1 *Exploring the photochemical roles of excited singlet and triplet states*

To estimate whether the excited singlet or triplet state of the reactant is a suitable product precursor, we compare the emission lifetimes with the relaxation time, τ, of the reactant due to the chemical reaction. As an illustration, consider a unimolecular photochemical reaction with rate constant $k = 1.7 \times 10^4\ s^{-1}$ and relaxation time $\tau = 1/(1.7 \times 10^4\ s^{-1}) = 59\ \mu s$ that involves a reactant with an observed fluorescence lifetime of 1.0 ns and an observed phosphorescence lifetime of 1.0 ms. The excited singlet state is too short-lived and is not expected to be a major source of product in this reaction. On the other hand, the excited triplet state is a good candidate for a precursor.

(b) The primary quantum yield

We shall see that the rates of deactivation of the excited state by radiative, non-radiative, and chemical processes determine the yield of product in a photochemical reaction. The **primary quantum yield**, ϕ, is defined as the number of photophysical or photochemical events that lead to primary products divided by the number of photons absorbed by the molecule in the same interval. It follows that the primary quantum yield is also the rate of radiation-induced primary events divided by the rate of photon absorption. Because the rate of photon absorption is equal to the intensity of light absorbed by the molecule (Section 13.2), we write

$$\phi = \frac{\text{number of events}}{\text{number of photons absorbed}} = \frac{\text{rate of process}}{\text{intensity of light absorbed}} = \frac{v}{I_{\text{abs}}} \qquad [23.28]$$

A molecule in an excited state must either decay to the ground state or form a photochemical product. Therefore, the total number of molecules deactivated by radiative processes, non-radiative processes, and photochemical reactions must be equal to the number of excited species produced by absorption of light. We conclude that the sum of primary quantum yields ϕ_i for *all* photophysical and photochemical events i must be equal to 1, regardless of the number of reactions involving the excited state. It follows that

$$\sum_i \phi_i = \sum_i \frac{v_i}{I_{\text{abs}}} = 1 \qquad (23.29)$$

It follows that for an excited singlet state that decays to the ground state only via the photophysical processes described in Section 23.7(a), we write

$$\phi_{\text{f}} + \phi_{\text{IC}} + \phi_{\text{ISC}} + \phi_{\text{p}} = 1$$

where ϕ_f, ϕ_{IC}, ϕ_{ISC}, and ϕ_p are the quantum yields of fluorescence, internal conversion, intersystem crossing, and phosphorescence, respectively. The quantum yield of photon emission by fluorescence and phosphorescence is $\phi_{emission} = \phi_f + \phi_p$, which is less than 1. If the excited singlet state also participates in a primary photochemical reaction with quantum yield ϕ_R, we write

$$\phi_f + \phi_{IC} + \phi_{ISC} + \phi_p + \phi_R = 1$$

We can now strengthen the link between reaction rates and primary quantum yield already established by eqns 23.28 and 23.29. By taking the constant I_{abs} out of the summation in eqn 23.29 and rearranging, we obtain $I_{abs} = \sum_i v_i$. Substituting this result into eqn 23.29 gives the general result

$$\phi_i = \frac{v_i}{\sum_i v_i} \tag{23.30}$$

Therefore, the primary quantum yield may be determined directly from the experimental rates of *all* photophysical and photochemical processes that deactivate the excited state.

(c) Mechanism of decay of excited singlet states

Consider the formation and decay of an excited singlet state in the absense of a chemical reaction:

Absorption:	$S + h\nu_i \rightarrow S^*$	$v_{abs} = I_{abs}$
Fluorescence:	$S^* \rightarrow S + h\nu_f$	$v_f = k_f[S^*]$
Internal conversion:	$S^* \rightarrow S$	$v_{IC} = k_{IC}[S^*]$
Intersystem crossing:	$S^* \rightarrow T^*$	$v_{ISC} = k_{ISC}[S^*]$

in which S is an absorbing species, S* an excited singlet state, T* an excited triplet state, and $h\nu_i$ and $h\nu_f$ are the energies of the incident and fluorescent photons, respectively. From the methods developed in Chapter 22 and the rates of the steps that form and destroy the excited singlet state S*, we write the rate of formation and decay of S* as:

$$\textit{Rate of formation of } [S^*] = I_{abs}$$

$$\textit{Rate of decay of } [S^*] = -k_f[S^*] - k_{ISC}[S^*] - k_{IC}[S^*] = -(k_f + k_{ISC} + k_{IC})[S^*]$$

It follows that the excited state decays by a first-order process so, when the light is turned off, the concentration of S* varies with time t as:

$$[S^*]_t = [S^*]_0 e^{-t/\tau_0} \tag{23.31}$$

where the **observed fluorescence lifetime**, τ_0, is defined as:

$$\tau_0 = \frac{1}{k_f + k_{ISC} + k_{IC}} \tag{23.32}$$

We show in the following *Justification* that the quantum yield of fluorescence is

$$\phi_f = \frac{k_f}{k_f + k_{ISC} + k_{IC}} \tag{23.33}$$

Justification 23.4 *The quantum yield of fluorescence*

Most fluorescence measurements are conducted by illuminating a relatively dilute sample with a continuous and intense beam of light. It follows that [S*] is small and constant, so we may invoke the steady-state approximation (Section 22.7) and write:

$$\frac{d[S^*]}{dt} = I_{abs} - k_f[S^*] - k_{ISC}[S^*] - k_{IC}[S^*] = I_{abs} - (k_f + k_{ISC} + k_{IC})[S^*] = 0$$

Consequently,

$$I_{abs} = (k_f + k_{ISC} + k_{IC})[S^*]$$

By using this expression and eqn 23.28, the quantum yield of fluorescence is written as:

$$\phi_f = \frac{v_f}{I_{abs}} = \frac{k_f[S^*]}{(k_f + k_{ISC} + k_{IC})[S^*]}$$

which, by cancelling the [S*], simplifies to eqn 23.33.

The observed fluorescence lifetime can be measured with a pulsed laser technique (Section 13.12b). First, the sample is excited with a short light pulse from a laser using a wavelength at which S absorbs strongly. Then, the exponential decay of the fluorescence intensity after the pulse is monitored. From eqn 13.28, it follows that

$$\tau_0 = \frac{1}{k_f + k_{ISC} + k_{IC}} = \left(\frac{k_f}{k_f + k_{ISC} + k_{IC}}\right) \times \frac{1}{k_f} = \frac{\phi_f}{k_f} \tag{23.34}$$

Illustration 23.2 *Calculating the fluorescence rate constant of tryptophan*

In water, the fluorescence quantum yield and observed fluorescence lifetime of tryptophan are $\phi_f = 0.20$ and $\tau_0 = 2.6$ ns, respectively. It follows from eqn 23.33 that the fluorescence rate constant k_f is

$$k_f = \frac{\phi_f}{\tau_0} = \frac{0.20}{2.6 \times 10^{-9}\ s} = 7.7 \times 10^7\ s^{-1}$$

(d) Quenching

The shortening of the lifetime of the excited state is called **quenching**. Quenching may be either a desired process, such as in energy or electron transfer, or an undesired side reaction that can decrease the quantum yield of a desired photochemical process. Quenching effects may be studied by monitoring the emission from the excited state that is involved in the photochemical reaction.

The addition of a quencher, Q, opens an additional channel for deactivation of S*:

Quenching: $S^* + Q \rightarrow S + Q \qquad v_Q = k_Q[Q][S^*]$

The **Stern–Volmer equation**, which is derived in the *Justification* below, relates the fluorescence quantum yields $\phi_{f,0}$ and ϕ_f measured in the absence and presence, respectively, of a quencher Q at a molar concentration [Q]:

$$\frac{\phi_{f,0}}{\phi_f} = 1 + \tau_0 k_Q[Q] \tag{23.35}$$

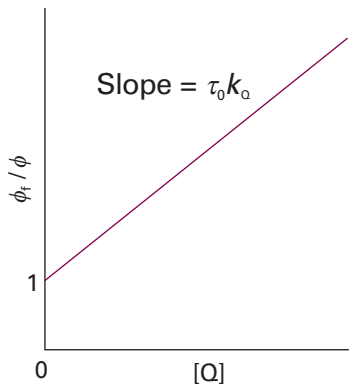

Fig. 23.14 The format of a Stern–Volmer plot and the interpretation of the slope in terms of the rate constant for quenching and the observed fluorescence lifetime in the absence of quenching.

This equation tells us that a plot of $\phi_{f,0}/\phi_f$ against [Q] should be a straight line with slope $\tau_0 k_Q$. Such a plot is called a **Stern–Volmer plot** (Fig. 23.14). The method may also be applied to the quenching of phosphorescence.

Justification 23.5 *The Stern–Volmer equation*

With the addition of quenching, the steady-state approximation for [S*] now gives:

$$\frac{d[S^*]}{dt} = I_{abs} - (k_f + k_{IC} + k_{ISC} + k_{IC} + k_Q[Q])[S^*] = 0$$

and the fluorescence quantum yield in the presence of the quencher is:

$$\phi_f = \frac{k_f}{k_f + k_{ISC} + k_{IC} + k_Q[Q]}$$

When [Q] = 0, the quantum yield is

$$\phi_{f,0} = \frac{k_f}{k_f + k_{ISC} + k_{IC}}$$

It follows that

$$\frac{\phi_{f,0}}{\phi_f} = \left(\frac{k_f}{k_f + k_{ISC} + k_{IC}}\right) \times \left(\frac{k_f + k_{ISC} + k_{IC} + k_Q[Q]}{k_f}\right)$$

$$= \frac{k_f + k_{ISC} + k_{IC} + k_Q[Q]}{k_f + k_{ISC} + k_{IC}}$$

$$= 1 + \frac{k_Q}{k_f + k_{ISC} + k_{IC}}[Q]$$

By using eqn 23.34, this expression simplifies to eqn 23.35.

Because the fluorescence intensity and lifetime are both proportional to the fluorescence quantum yield (specifically, from eqn 23.34, $\tau = \phi_f/k_f$), plots of $I_{f,0}/I_f$ and τ_0/τ (where the subscript 0 indicates a measurement in the absence of quencher) against [Q] should also be linear with the same slope and intercept as those shown for eqn 23.35.

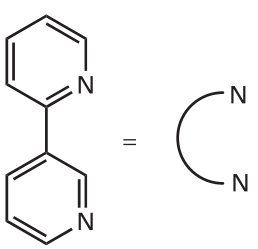

1 2,2′-Bipyridine (bipy)

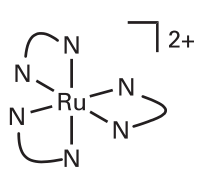

2

Example 23.4 *Determining the quenching rate constant*

The molecule 2,2′-bipyridine (**1**) forms a complex with the Ru^{2+} ion. Ruthenium(II) tris-(2,2′-bipyridyl), $Ru(bipy)_3^{2+}$ (**2**), has a strong metal-to-ligand charge transfer (MLCT) transition (Section 14.2) at 450 nm. The quenching of the $^*Ru(bipy)_3^{2+}$ excited state by $Fe(H_2O)_6^{3+}$ in acidic solution was monitored by measuring emission lifetimes at 600 nm. Determine the quenching rate constant for this reaction from the following data:

$[Fe(H_2O)_6^{3+}]/(10^{-4}\ mol\ dm^{-3})$	0	1.6	4.7	7	9.4
$t/(10^{-7}\ s)$	6	4.05	3.37	2.96	2.17

Method Re-write the Stern–Volmer equation (eqn 23.35) for use with lifetime data then fit the data to a straight-line.

Answer Upon substitution of τ_0/τ for $\phi_{0,f}/\phi_f$ in eqn 23.35 and after rearrangement, we obtain:

$$\frac{1}{\tau}=\frac{1}{\tau_0}+k_Q[Q] \qquad (23.36)$$

Figure 23.15 shows a plot of $1/\tau$ versus $[Fe^{3+}]$ and the results of a fit to eqn 23.36. The slope of the line is 2.8×10^9, so $k_Q = 2.8\times10^9$ dm^3 mol^{-1} s^{-1}.

This example shows that measurements of emission lifetimes are preferred because they yield the value of k_Q directly. To determine the value of k_Q from intensity or quantum yield measurements, we need to make an independent measurement of τ_0.

Self-test 23.4 The quenching of tryptophan fluorescence by dissolved O_2 gas was monitored by measuring emission lifetimes at 348 nm in aqueous solutions. Determine the quenching rate constant for this process from the following data:

$[O_2]/(10^{-2}$ mol dm$^{-3})$	0	2.3	5.5	8	10.8
$\tau/(10^{-9}$ s)	2.6	1.5	0.92	0.71	0.57

[1.3×10^{10} dm^3 mol^{-1} s^{-1}]

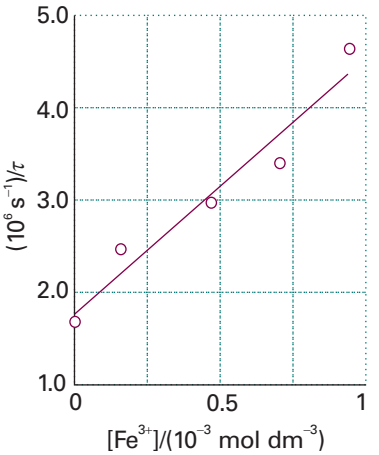

Fig. 23.15 The Stern–Volmer plot of the data for Example 23.4.

Three common mechanisms for bimolecular quenching of an excited singlet (or triplet) state are:

Collisional deactivation:	$S^* + Q \rightarrow S + Q$
Resonance energy transfer:	$S^* + Q \rightarrow S + Q^*$
Electron transfer:	$S^* + Q \rightarrow S^+ + Q^-$ or $S^- + Q^+$

Collisional quenching is particularly efficient when Q is a heavy species, such as iodide ion, which receives energy from S* and then decays primarily by internal conversion to the ground state. This fact may be used to determine the accessibility of amino acid residues of a folded protein to solvent. For example, fluorescence from a tryptophan residue ($\lambda_{abs} \approx 290$ nm, $\lambda_{fluor} \approx 350$ nm) is quenched by iodide ion when the residue is on the surface of the protein and hence accessible to the solvent. Conversely, residues in the hydrophobic interior of the protein are not quenched effectively by I^-.

The quenching rate constant itself does not give much insight into the mechanism of quenching. For the system of Example 23.4, it is known that the quenching of the excited state of $Ru(bipy)_3^{2+}$ is a result of light-induced electron transfer to Fe^{3+}, but the quenching data do not allow us to prove the mechanism. However, there are some criteria that govern the relative efficiencies of energy and electron transfer.

(e) Resonance energy transfer

We visualize the process $S^* + Q \rightarrow S + Q^*$ as follows. The oscillating electric field of the incoming electromagnetic radiation induces an oscillating electric dipole moment in S. Energy is absorbed by S if the frequency of the incident radiation, ν, is such that $\nu = \Delta E_S/h$, where ΔE_S is the energy separation between the ground and excited electronic states of S and h is Planck's constant. This is the 'resonance condition' for absorption of radiation. The oscillating dipole on S now can affect electrons bound to a nearby Q molecule by inducing an oscillating dipole moment in the latter. If the frequency of oscillation of the electric dipole moment in S is such that $\nu = \Delta E_Q/h$ then Q will absorb energy from S.

The efficiency, E_T, of resonance energy transfer is defined as

$$E_T = 1 - \frac{\phi_f}{\phi_{f,0}} \qquad [23.37]$$

Table 23.3 Values of R_0 for some donor–acceptor pairs*

Donor†	Acceptor	R_0/nm
Naphthalene	Dansyl	2.2
Dansyl	ODR	4.3
Pyrene	Coumarin	3.9
IEDANS	FITC	4.9
Tryptophan	IEDANS	2.2
Tryptophan	Haem (heme)	2.9

* Additional values may be found in J.R. Lacowicz in *Principles of fluorescence spectroscopy*, Kluwer Academic/Plenum, New York (1999).
† Abbreviations: Dansyl, 5-dimethylamino-1-naphthalenesulfonic acid; FITC, fluorescein 5-isothiocyanate; IEDANS, 5-((((2-iodoacetyl)amino)ethyl)amino)naphthalene-1-sulfonic acid; ODR, octadecyl-rhodamine.

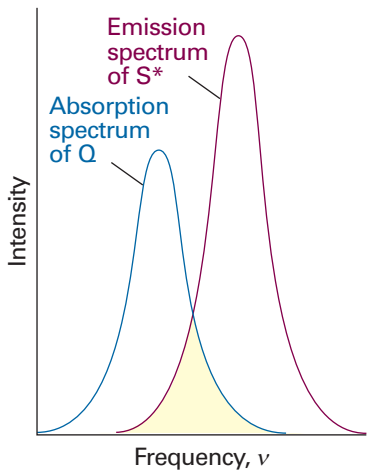

Fig. 23.16 According to the Förster theory, the rate of energy transfer from a molecule S* in an excited state to a quencher molecule Q is optimized at radiation frequencies in which the emission spectrum of S* overlaps with the absorption spectrum of Q, as shown in the shaded region.

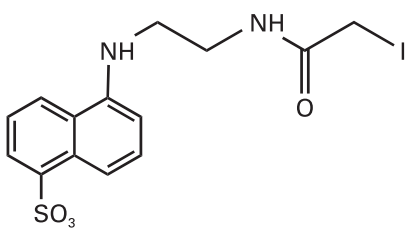

3 1.5-I AEDANS

According to the **Förster theory** of resonance energy transfer, which was proposed by T. Förster in 1959, energy transfer is efficient when:

1 The energy donor and acceptor are separated by a short distance (of the order of nanometres).

2 Photons emitted by the excited state of the donor can be absorbed directly by the acceptor.

We show in *Further information* 23.1 that for donor–acceptor systems that are held rigidly either by covalent bonds or by a protein 'scaffold', E_T increases with decreasing distance, R, according to

$$E_T = \frac{R_0^6}{R_0^6 + R^6} \tag{23.38}$$

where R_0 is a parameter (with units of distance) that is characteristic of each donor–acceptor pair. Equation 23.38 has been verified experimentally and values of R_0 are available for a number of donor–acceptor pairs (Table 23.3).

The emission and absorption spectra of molecules span a range of wavelengths, so the second requirement of the Förster theory is met when the emission spectrum of the donor molecule overlaps significantly with the absorption spectrum of the acceptor. In the overlap region, photons emitted by the donor have the proper energy to be absorbed by the acceptor (Fig. 23.16).

In many cases, it is possible to prove that energy transfer is the predominant mechanism of quenching if the excited state of the acceptor fluoresces or phosphoresces at a characteristic wavelength. In a pulsed laser experiment, the rise in fluorescence intensity from Q* with a characteristic time that is the same as that for the decay of the fluorescence of S* is often taken as indication of energy transfer from S to Q.

Equation 23.38 forms the basis of **fluorescence resonance energy transfer** (FRET), in which the dependence of the energy transfer efficiency, E_T, on the distance, R, between energy donor and acceptor can be used to measure distances in biological systems. In a typical FRET experiment, a site on a biopolymer or membrane is labelled covalently with an energy donor and another site is labelled covalently with an energy acceptor. In certain cases, the donor or acceptor may be natural constituents of the system, such as amino acid groups, cofactors, or enzyme substrates. The distance between the labels is then calculated from the known value of R_0 and eqn 23.38. Several tests have shown that the FRET technique is useful for measuring distances ranging from 1 to 9 nm.

Illustration 23.3 *Using FRET analysis*

As an illustration of the FRET technique, consider a study of the protein rhodopsin (*Impact* I14.1). When an amino acid on the surface of rhodopsin was labelled covalently with the energy donor 1.5-I AEDANS (**3**), the fluorescence quantum yield of the label decreased from 0.75 to 0.68 due to quenching by the visual pigment 11-*cis*-retinal (**4**). From eqn 23.37, we calculate $E_T = 1 - (0.68/0.75) = 0.093$ and from eqn 23.38 and the known value of $R_0 = 5.4$ nm for the 1.5-I AEDANS/11-*cis*-retinal pair we calculate $R = 7.9$ nm. Therefore, we take 7.9 nm to be the distance between the surface of the protein and 11-*cis*-retinal.

If donor and acceptor molecules diffuse in solution or in the gas phase, Förster theory predicts that the efficiency of quenching by energy transfer increases as the

average distance travelled between collisions of donor and acceptor decreases. That is, the quenching efficiency increases with concentration of quencher, as predicted by the Stern–Volmer equation.

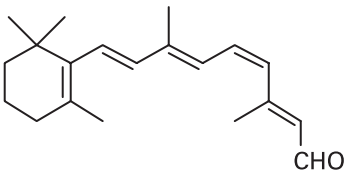

4 11-*cis*-retinal

(f) Electron transfer reactions

According to the **Marcus theory** of electron transfer, which was proposed by R.A. Marcus in 1965 and is discussed fully in Section 24.11, the rates of electron transfer (from ground or excited states) depend on:

1 The distance between the donor and acceptor, with electron transfer becoming more efficient as the distance between donor and acceptor decreases.

2 The reaction Gibbs energy, $\Delta_r G$, with electron transfer becoming more efficient as the reaction becomes more exergonic. For example, efficient photooxidation of S requires that the reduction potential of S* be lower than the reduction potential of Q.

3 The reorganization energy, the energy cost incurred by molecular rearrangements of donor, acceptor, and medium during electron transfer. The electron transfer rate is predicted to increase as this reorganization energy is matched closely by the reaction Gibbs energy.

Electron transfer can also be studied by time-resolved spectroscopy (Section 14.6). The oxidized and reduced products often have electronic absorption spectra distinct from those of their neutral parent compounds. Therefore, the rapid appearance of such known features in the absorption spectrum after excitation by a laser pulse may be taken as indication of quenching by electron transfer.

IMPACT ON ENVIRONMENTAL SCIENCE

I23.1 The chemistry of stratospheric ozone

The Earth's atmosphere contains primarily N_2 and O_2 gas, with low concentrations of a large number of other species of both natural and anthropogenic origins. Indeed, many of the natural trace constituents of our atmosphere participate in complex chemical reactions that have contributed to the proliferation of life on the planet. The development of industrial societies has added new components to the Earth's atmosphere and has led to significant changes in the concentrations of some natural trace species. The negative consequences of these changes for the environment are either already being felt or, more disturbingly, are yet to be felt in the next few decades (see, for example, the discussion of global warming in *Impact* I13.2). Careful kinetic analysis allows us to understand the origins of our complex atmosphere and point to ways in which environmental problems can be solved or avoided.

The Earth's atmosphere consists of layers, as shown in Fig. 23.17. The pressure decreases as altitude increases (see Problems 1.27 and 16.20), but the variation of temperature with altitude is complex, owing to processes that capture radiant energy from the Sun. We focus on the *stratosphere*, a region spanning from 15 km to 50 km above the surface of the Earth, and on the chemistry of the trace component ozone, O_3.

In the *troposphere*, the region between the Earth's surface and the stratosphere, temperature decreases with increasing altitude. This behaviour may be understood in terms of a model in which the boundary between the troposphere and the stratosphere, also called the *tropopause*, is considered adiabatic. Then we know from Section 2.6 that, as atmospheric gases are allowed to expand from layers close to the surface to higher layers, the temperature varies with pressure, and hence height, as

$$\frac{T_{\text{low altitude}}}{T_{\text{high altitude}}} = \left(\frac{p_{\text{low altitude}}}{p_{\text{high altitude}}}\right)^{c} \qquad c = \frac{C_{p,\text{m}}}{C_{V,\text{m}}} - 1$$

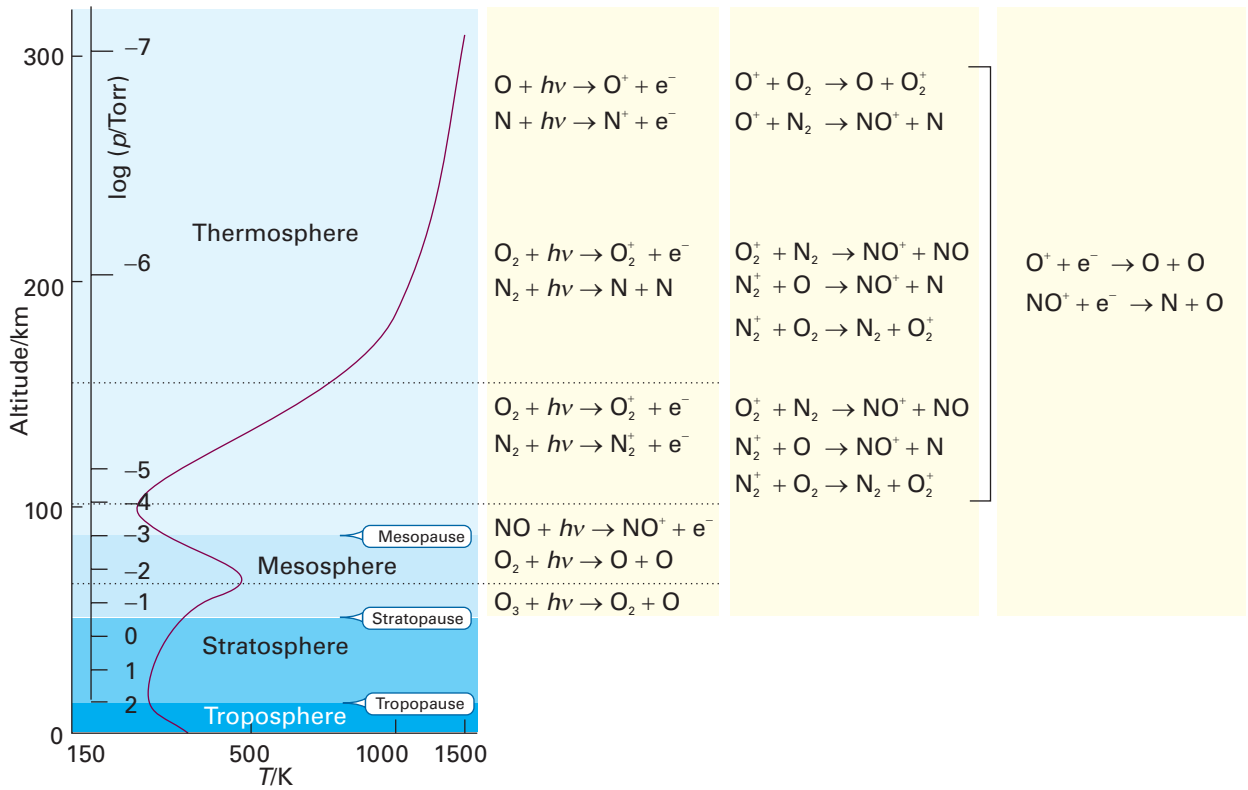

Fig. 23.17 The temperature profile through the atmosphere and some of the reactions that occur in each region.

The model predicts a decrease in temperature with increasing altitude because $C_{p,\mathrm{m}}/C_{V,\mathrm{m}} \approx \frac{7}{5}$ for air. In the stratosphere, a *temperature inversion* is observed because of photochemical chain reactions that produce ozone from O_2. The *Chapman model* accounts for ozone formation and destruction in an atmosphere that contains only O_2:

Initiation:	$O_2 + h\nu \rightarrow O + O$	$185\ \mathrm{nm} < \lambda < 220\ \mathrm{nm}$	$v = k_1[O_2]$
Propagation:	$O + O_2 + M \rightarrow O_3 + M^*$	$\Delta_r H = -106.6\ \mathrm{kJ\ mol^{-1}}$	$v = k_2[O][O_2][M]$
	$O_3 + h\nu \rightarrow O_2 + O$	$210\ \mathrm{nm} < \lambda < 300\ \mathrm{nm}$	$v = k_3[O_3]$
Termination:	$O + O_3 \rightarrow O_2 + O_2$	$\Delta_r H = -391.9\ \mathrm{kJ\ mol^{-1}}$	$v = k_4[O][O_3]$
	$O + O + M \rightarrow O_2 + M^*$		$v = k_5[O]^2[M]$

where M is an arbitrary third body, such as O_2 in an 'oxygen-only' atmosphere, which helps to remove excess energy from the products of combination and recombination reactions. The mechanism shows that absorption of radiation by O_2 and O_3 during the daytime leads to the production of reactive O atoms, which, in turn, participate in exothermic reactions that are responsible for the heating of the stratosphere.

Using values of the rate constants that are applicable to stratospheric conditions, the Chapman model predicts a net formation of trace amounts of ozone, as seen in Fig. 23.18 (see also Problem 23.33). However, the model overestimates the concentration of ozone in the stratosphere because other trace species X contribute to catalytic enhancement of the termination step $O_3 + O \rightarrow O_2 + O_2$ according to

$$X + O_3 \rightarrow XO + O_2$$
$$XO + O \rightarrow X + O_2$$

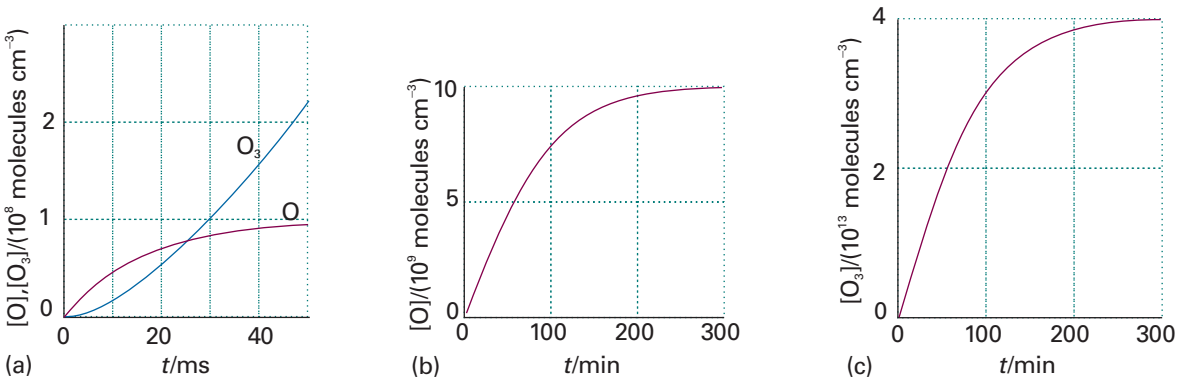

Fig. 23.18 Net formation of ozone via the Chapman model in a stratospheric model containing only O_2, O, andO_3. The rate constants are consistent with reasonable stratospheric conditions. (a) Early reaction period after irradiation begins at $t = 0$. (b) Late reaction period, showing that the concentration of O atoms begins to level off after about 4 hours of continuous irradiation. (c) Late reaction period, showing that the ozone concentration also begins to level off similarly. For details of the calculation, see Problem 23.33 and M.P. Cady and C.A. Trapp, *A Mathcad primer for physical chemistry*. Oxford University Press (1999).

The catalyst X can be H, OH, NO, or Cl. Chlorine atoms are produced by photolysis of CH_3Cl which, in turn, is a by-product of reactions between Cl^- and decaying vegetation in oceans. Nitric oxide, NO, is produced in the stratosphere from reaction between excited oxygen atoms and N_2O, which is formed mainly by microbial denitrification processes in soil. The hydroxyl radical is a product, along with the methyl radical, of the reaction between excited oxygen atoms and methane gas, which is a by-product of a number of natural processes (such as digestion of cellulose in ruminant animals, anaerobic decomposition of organic waste matter) and industrial processes (such as food production and fossil fuel use). In spite of the presence of these catalysts, a natural stratosphere is still capable to maintain a low concentration of ozone.

The chemistry outlined above shows that the photochemical reactions of the Chapman model account for absorption of a significant portion of solar ultraviolet radiation in the stratosphere. Hence, the surface of the Earth is bathed by lower energy radiation, which does not damage biological tissue (see *Impact* I23.3). However, some pollutants can lower the concentration of stratospheric ozone. For example, chlorofluorocarbons (CFCs) have been used as propellants and refrigerants over many years. As CFC molecules diffuse slowly into the middle stratosphere, they are finally photolysed by ultraviolet radiation. For CF_2Cl_2, also known as CFC-12, the reaction is:

$$CF_2Cl_2 + h\nu \rightarrow CF_2Cl + Cl$$

We already know that the resulting Cl atoms can participate in the decomposition of ozone according to the catalytic cycle shown in Fig. 23.19. A number of experimental observations have linked this chemistry of CFCs to a dangerously rapid decline in the concentration of stratospheric ozone over the last three decades.

Ozone depletion has increased the amount of ultraviolet radiation at the Earth's surface, particularly radiation in the 'UVB range', 290–320 nm. The physiological consequences of prolonged exposure to UVB radiation include DNA damage, principally by photodimerization of adjacent thymine bases to yield either a cyclobutane

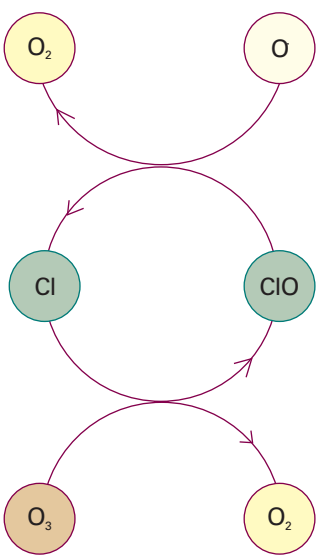

Fig. 23.19 A catalytic cycle showing the propagation of ozone decomposition by chlorine atoms.

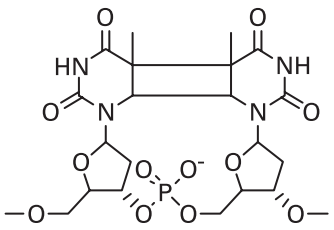

5

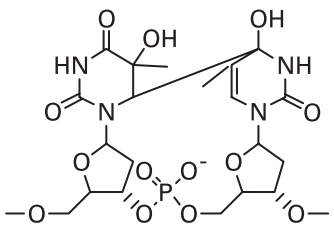

6

thymine dimer (**5**) or a so-called 6–4 photoproduct (**6**). The former has been linked directly to cell death and the latter may lead to DNA mutations and, consequently, to the formation of tumours. There are several natural mechanisms for protection from and repair of photochemical damage. For example, the enzyme DNA photolyase, present in organisms from all kingdoms but not in humans, catalyses the destruction of cyclobutane thymine dimers. Also, ultraviolet radiation can induce the production of the pigment melanin (in a process more commonly known as 'tanning'), which shields the skin from damage. However, repair and protective mechanisms become increasingly less effective with persistent and prolonged exposure to solar radiation. Consequently, there is concern that the depletion of stratospheric ozone may lead to an increase in mortality not only of animals but also the plants and lower organisms that form the base of the food chain.

Chlorofluorocarbons are being phased out according to international agreements and alternatives, such as the hydrofluorocarbon CH_2FCH_3, are already being used. However, the temperature inversion shown in Fig. 23.17 leads to trapping of gases in the troposphere, so CFCs are likely to continue to cause ozone depletion over many decades as the molecules diffuse slowly into the middle stratosphere, where they are photolysed by intense solar UV radiation.

IMPACT ON BIOCHEMISTRY

I23.2 Harvesting of light during plant photosynthesis

A large proportion of solar radiation with wavelengths below 400 nm and above 1000 nm is absorbed by atmospheric gases such as ozone and O_2, which absorb ultraviolet radiation (*Impact* I23.1), and CO_2 and H_2O, which absorb infrared radiation (*Impact* I13.2). As a result, plants, algae, and some species of bacteria evolved photosynthetic apparatus that capture visible and near-infrared radiation. Plants use radiation in the wavelength range of 400–700 nm to drive the endergonic reduction of CO_2 to glucose, with concomitant oxidation of water to O_2 ($\Delta_r G^{\oplus} = +2880$ kJ mol^{-1}), in essence the reverse of glycolysis and the citric acid cycle (*Impact* I7.2):

$$6\,CO_2(g) + 6\,H_2O(l) \underset{\text{glycolysis and the citric acid cycle}}{\overset{\text{photosynthesis}}{\rightleftharpoons}} C_6H_{12}O_6(s) + 6\,O_2(g)$$

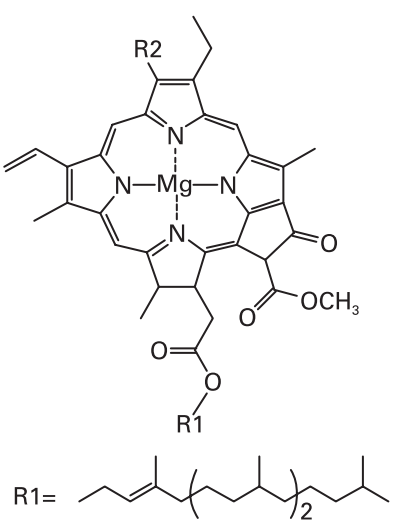

7 Chlorophyll *a* and *b*

Electrons flow from reductant to oxidant via a series of electrochemical reactions that are coupled to the synthesis of ATP. The process takes place in the *chloroplast*, a special organelle of the plant cell, where chlorophylls *a* and *b* (**7**) and carotenoids (of which *β*-carotene, **8**, is an example) bind to integral proteins called *light harvesting complexes*, which absorb solar energy and transfer it to protein complexes known as *reaction centres*, where light-induced electron transfer reactions occur. The combination of a light harvesting complex and a reaction centre complex is called a photosystem. Plants have two photosystems that drive the reduction of $NADP^+$ (**9**) by water:

$$2\,H_2O + 2\,NADP^+ \xrightarrow{\text{light, photosystems I and II}} O_2 + 2\,NADPH + 2\,H^+$$

It is clear that energy from light is required to drive this reaction because, in the dark, $E^{\oplus} = -1.135$ V and $\Delta_r G^{\oplus} = +438.0$ kJ mol^{-1}.

Light harvesting complexes bind large numbers of pigments in order to provide a sufficiently large area for capture of radiation. In photosystems I and II, absorption of a photon raises a chlorophyll or carotenoid molecule to an excited singlet state and within 0.1–5 ps the energy hops to a nearby pigment via the Förster mechanism (Section 23.7e). About 100–200 ps later, which corresponds to thousands of hops within the light harvesting complex, more than 90 per cent of the absorbed energy reaches the reaction centre. There, a chlorophyll *a* dimer becomes electronically

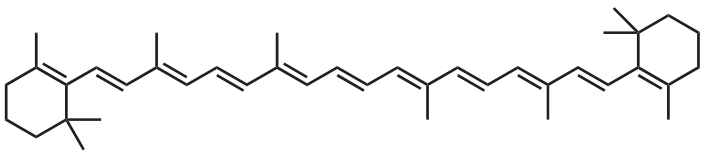

8 β-Carotene

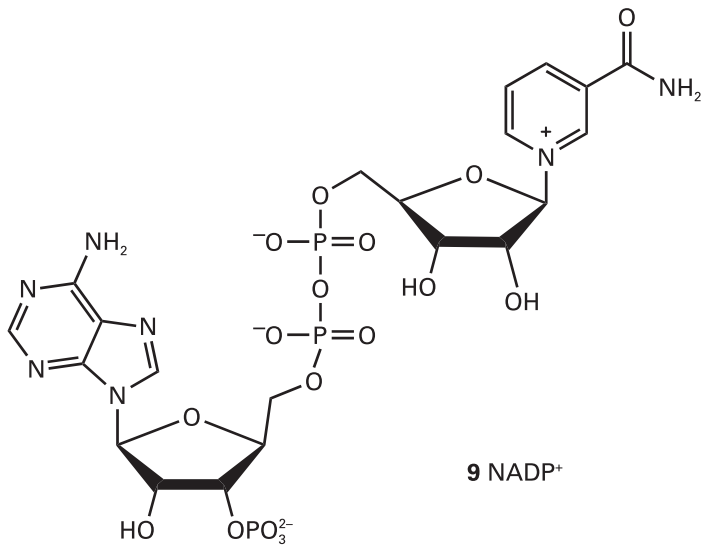

9 $NADP^+$

excited and initiates ultrafast electron transfer reactions. For example, the transfer of an electron from the excited singlet state of P680, the chlorophyll dimer of the photosystem II reaction centre, to its immediate electron acceptor, a phaeophytin *a* molecule (a chlorophyll *a* molecule where the central Mg^{2+} ion is replaced by two protons, which are bound to two of the pyrrole nitrogens in the ring), occurs within 3 ps. Once the excited state of P680 has been quenched efficiently by this first reaction, subsequent steps that lead to the oxidation of water occur more slowly, with reaction times varying from 200 ps to 1 ms. The electrochemical reactions within the photosystem I reaction centre also occur in this time interval. We see that the initial energy and electron transfer events of photosynthesis are under tight kinetic control. Photosynthesis captures solar energy efficiently because the excited singlet state of chlorophyll is quenched rapidly by processes that occur with relaxation times that are much shorter than the fluorescence lifetime, which is typically about 1 ns in organic solvents at room temperature.

Working together, photosystem I and the enzyme ferredoxin:$NADP^+$ oxidoreductase catalyse the light-induced oxidation of $NADP^+$ to NADPH. The electrons required for this process come initially from P700 in its excited state. The resulting $P700^+$ is then reduced by the mobile carrier plastocyanin (Pc), a protein in which the bound copper ion can exist in oxidation states +2 and +1. The net reaction is

$$NADP^+ + 2\,Cu^+(Pc) + H^+ \xrightarrow{\text{light, photosystem I}} NADPH + 2\,Cu^{2+}(Pc)$$

Oxidized plastocyanin accepts electrons from reduced plastoquinone (PQ, **10**). The process is catalysed by the cytochrome b_6f complex, a membrane protein complex that resembles complex III of mitochondria (*Impact* I7.2):

$$PQH_2 + 2\,Cu^{2+}(Pc) \xrightarrow{\text{cyt } b_6f \text{ complex}} PQ + 2\,H^+ + 2\,Cu^+(Pc)$$

$$E^\oplus = +0.370\ V,\ \Delta_r G^\oplus = -71.4\ kJ\ mol^{-1}$$

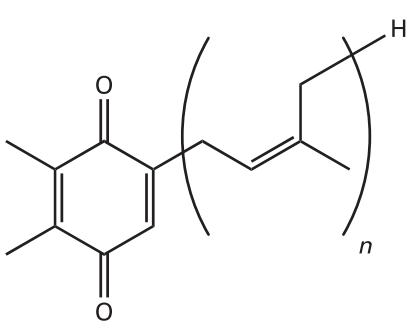

10 Plastoquinone

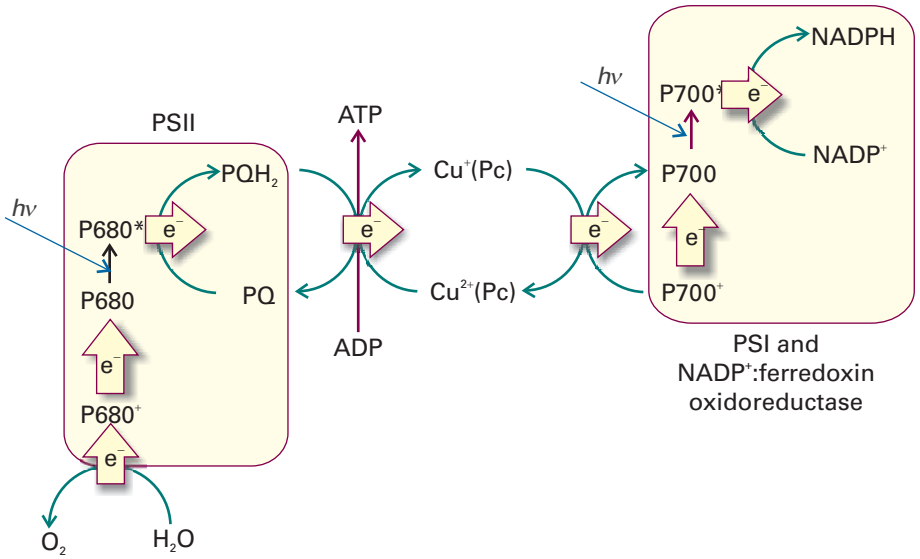

Fig. 23.20 In plant photosynthesis, light-induced electron transfer processes lead to the oxidation of water to O_2 and the reduction of $NADP^+$ to NADPH, with concomitant production of ATP. The energy stored in ATP and NADPH is used to reduce CO_2 to carbohydrate in a separate set of reactions. The scheme summarizes the general patterns of electron flow and does not show all the intermediate electron carriers in photosystems I and II, the cytochrome b_6f complex, and ferredoxin:$NADP^+$ oxidoreductase.

This reaction is sufficiently exergonic to drive the synthesis of ATP in the process known as **photophosphorylation**.

Plastoquinone is reduced by water in a process catalysed by light and photosystem II. The electrons required for the reduction of plastoquinone come initially from P680 in its excited state. The resulting $P680^+$ is then reduced ultimately by water. The net reaction is

$$H_2O + PQ \xrightarrow{\text{light, photosystem II}} \tfrac{1}{2}O_2 + PQH_2$$

In this way, plant photosynthesis uses an abundant source of electrons (water) and of energy (the Sun) to drive the endergonic reduction of $NADP^+$, with concomitant synthesis of ATP (Fig. 23.20). Experiments show that, for each molecule of NADPH formed in the chloroplast of green plants, one molecule of ATP is synthesized.

The ATP and NADPH molecules formed by the light-induced electron transfer reactions of plant photosynthesis participate directly in the reduction of CO_2 to glucose in the chloroplast:

$$6\,CO_2 + 12\,NADPH + 12\,ATP + 12\,H^+ \rightarrow C_6H_{12}O_6 + 12\,NADP^+ + 12\,ADP + 12\,P_i + 6H_2O$$

In summary, plant photosynthesis uses solar energy to transfer electrons from a poor reductant (water) to carbon dioxide. In the process, high energy molecules (carbohydrates, such as glucose) are synthesized in the cell. Animals feed on the carbohydrates derived from photosynthesis. During aerobic metabolism, the O_2 released by photosynthesis as a waste product is used to oxidize carbohydrates to CO_2, driving biological processes, such as biosynthesis, muscle contraction, cell division, and nerve conduction. Hence, the sustenance of life on Earth depends on a tightly regulated carbon–oxygen cycle that is driven by solar energy.

23.8 Complex photochemical processes

Many photochemical processes have complex mechanisms that may be examined by considering the concepts developed above. In this section, we consider two examples: photochemical chain reactions and photosensitization.

(a) The overall quantum yield of a photochemical reaction

For complex reactions involving secondary processes, such as chain reactions initiated by photolysis, many reactant molecules might be consumed as a result of absorption of a single photon. The **overall quantum yield**, Φ, for such reactions, the number of reactant molecules consumed per photon absorbed, might exceed 1. In the photolysis of HI, for example, the processes are

$$HI + h\nu \rightarrow H\cdot + I\cdot$$

$$H\cdot + HI \rightarrow H_2 + I\cdot$$

$$I\cdot + I\cdot + M \rightarrow I_2 + M^*$$

The overall quantum yield is 2 because the absorption of one photon leads to the destruction of two HI molecules. In a chain reaction, Φ may be very large, and values of about 10^4 are common. In such cases the chain acts as a chemical amplifier of the initial absorption step.

Example 23.5 *Determining the quantum yield of a photochemical reaction*

When a sample of 4-heptanone was irradiated for 100 s with 313 nm radiation with a power output of 50 W under conditions of total absorption, it was found that 2.8 mmol C_2H_4 was formed. What is the quantum yield for the formation of ethene?

Method First, calculate the amount of photons generated in an interval Δt: see Example 8.1. Then divide the amount of ethene molecules formed by the amount of photons absorbed.

Answer From Example 8.1, the amount (in moles) of photons absorbed is

$$n = \frac{P\Delta t}{(hc/\lambda)N_A}$$

If $n_{C_2H_4}$ is the amount of ethene formed, the quantum yield is

$$\Phi = \frac{n_{C_2H_4}}{n} = \frac{n_{C_2H_4} N_A hc}{\lambda P \Delta t}$$

$$= \frac{(2.8\times10^{-3}\ \text{mol})\times(6.022\times10^{23}\ \text{mol}^{-1})\times(6.626\times10^{-34}\ \text{J s})\times(2.997\times10^{8}\ \text{m s}^{-1})}{(3.13\times10^{-7}\ \text{m})\times(50\ \text{J s}^{-1})\times(100\ \text{s})}$$

$$= 0.21$$

Self-test 23.5 The overall quantum yield for another reaction at 290 nm is 0.30. For what length of time must irradiation with a 100 W source continue in order to destroy 1.0 mol of molecules? [3.8 h]

(b) Rate laws of complex photochemical reactions

As an example of how to write a rate law for a complex photochemical process, consider the photochemical activation of the reaction

$$H_2(g) + Br_2(g) \rightarrow 2\ HBr(g)$$

In place of the first step in the thermal reaction we have

$$Br_2 + h\nu \rightarrow Br\cdot + Br\cdot \qquad v = I_{abs}$$

where I_{abs} is the number of photons of the appropriate frequency absorbed divided by the volume in which absorption occurs and the time interval. We are assuming a

primary quantum yield of unity for the photodissociation of Br_2. It follows that I_{abs} should take the place of $k_i[Br_2][M]$ in the thermal reaction scheme, so from Example 23.1 we can write

$$\frac{d[HBr]}{dt} = \frac{2k_p(1/k_t[M])^{1/2}[H_2][Br_2]I_{abs}^{1/2}}{[Br_2] + (k_r/k'_p)[HBr]} \tag{23.39}$$

We predict that the reaction rate should depend on the square root of the absorbed light intensity, which is confirmed experimentally.

(c) Photosensitization

The reactions of a molecule that does not absorb directly can be made to occur if another absorbing molecule is present, because the latter may be able to transfer its energy to the former during a collision. An example of this **photosensitization** is the reaction used to generate excited state O_2 in a type of treatment known as *photodynamic therapy* (*Impact* I23.3). Another example is the reaction used to generate atomic hydrogen, the irradiation of hydrogen gas containing a trace of mercury vapour using radiation of wavelength 254 nm from a mercury discharge lamp. The Hg atoms are excited (to Hg*) by resonant absorption of the radiation, and then collide with H_2 molecules. Two reactions then take place:

$$Hg^* + H_2 \rightarrow Hg + H\cdot + H\cdot$$
$$Hg^* + H_2 \rightarrow HgH + H\cdot$$

The latter reaction is the initiation step for other mercury photosensitized reactions, such as the synthesis of formaldehyde from carbon monoxide and hydrogen:

$$H\cdot + CO \rightarrow HCO\cdot$$
$$HCO\cdot + H_2 \rightarrow HCHO + H\cdot$$
$$HCO\cdot + HCO\cdot \rightarrow HCHO + CO$$

Note that the last step is termination by disproportionation rather than by combination.

IMPACT ON MEDICINE

I23.3 Photodynamic therapy

In photodynamic therapy (PDT), laser radiation, which is usually delivered to diseased tissue through a fibre optic cable, is absorbed by a drug which, in its first excited triplet state ^3P, photosensitizes the formation of an excited singlet state of O_2, $^1O_2$. The $^1O_2$ molecules are very reactive and destroy cellular components and it is thought that cell membranes are the primary cellular targets. Hence, the photochemical cycle below leads to the shrinkage (and sometimes total destruction) of diseased tissue.

Absorption:	$P + h\nu \rightarrow P^*$
Intersystem crossing:	$P^* \rightarrow {}^3P$
Photosensitization:	$^3P + {}^3O_2 \rightarrow P + {}^1O_2$
Oxidation reactions:	$^1O_2$ + reactants $\rightarrow$ products

The photosensitizer is hence a 'photocatalyst' for the production of $^1O_2$. It is common practice to use a porphyrin photosensitizer, such as compounds derived from haematoporphyrin (**11**). However, much effort is being expended to develop better drugs with enhanced photochemical properties.

A potential PDT drug must meet many criteria. From the point of view of pharmacological effectiveness, the drug must be soluble in tissue fluids, so it can be transported to the diseased organ through blood and secreted from the body through

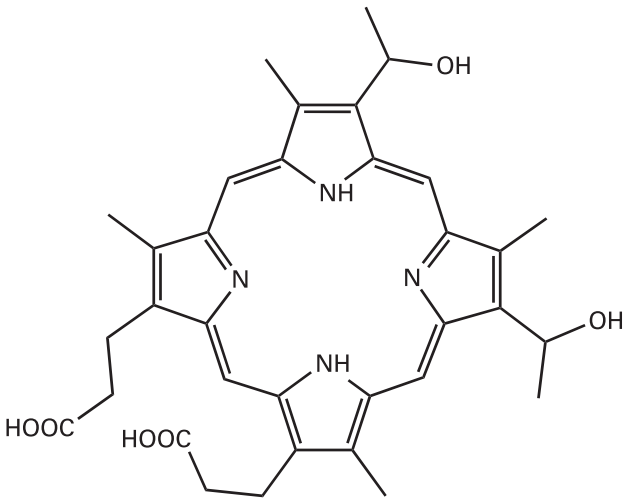

11 Haematoporphyrin

urine. The therapy should also result in very few side effects. The drug must also have unique photochemical properties. It must be activated photochemically at wavelengths that are not absorbed by blood and skin. In practice, this means that the drug should have a strong absorption band at $\lambda > 650$ nm. Drugs based on haematoporphyrin do not meet this criterion very well, so novel porphyrin and related macrocycles with more desirable electronic properties are being synthesized and tested. At the same time, the quantum yield of triplet formation and of $^1O_2$ formation must be high, so many drug molecules can be activated and many oxidation reactions can occur during a short period of laser irradiation. Photodynamic therapy has been used successfully in the treatment of macular degeneration, a disease of the retina that leads to blindness, and in a number of cancers, including those of the lung, bladder, skin, and oesophagus.

Checklist of key ideas

- ☐ 1. In a chain reaction, an intermediate (the chain carrier) produced in one step (the initiation step) attacks other reactant molecules (in the propagation steps), with each attack giving rise to a new carrier. The chain ends in the termination step. Examples of chain reactions include some explosions.
- ☐ 2. In stepwise polymerization any two monomers in the reaction mixture can link together at any time and growth of the polymer is not confined to chains that are already forming. The longer a stepwise polymerization proceeds, the higher the average molar mass of the product.
- ☐ 3. In chain polymerization an activated monomer attacks another monomer and links to it. That unit attacks another monomer, and so on. The slower the initiation of the chain, the higher the average molar mass of the polymer.
- ☐ 4. Catalysts are substances that accelerate reactions but undergo no net chemical change.
- ☐ 5. A homogeneous catalyst is a catalyst in the same phase as the reaction mixture. Enzymes are homogeneous, biological catalysts.
- ☐ 6. The Michaelis–Menten mechanism of enzyme kinetics accounts for the dependence of rate on the concentration of the substrate, $v = v_{max}[S]_0/([S]_0 + K_M)$.
- ☐ 7. A Lineweaver–Burk plot, based on $1/v = 1/v_{max} + (K_M/v_{max})(1/[S]_0)$, is used to determine the parameters that occur in the Michaelis–Menten mechanism.
- ☐ 8. In competitive inhibition of an enzyme, the inhibitor binds only to the active site of the enzyme and thereby inhibits the attachment of the substrate.
- ☐ 9. In uncompetitive inhibition the inhibitor binds to a site of the enzyme that is removed from the active site, but only if the substrate is already present.

☐ 10. In non-competitive inhibition, the inhibitor binds to a site other than the active site, and its presence reduces the ability of the substrate to bind to the active site.

☐ 11. The primary quantum yield of a photochemical reaction is the number of reactant molecules producing specified primary products for each photon absorbed; the overall quantum yield is the number of reactant molecules that react for each photon absorbed.

☐ 12. The observed fluorescence lifetime is related to the quantum yield, ϕ_f, and rate constant, k_f, of fluorescence by $\tau_0 = \phi_f/k_f$.

☐ 13. A Stern–Volmer plot is used to analyse the kinetics of fluorescence quenching in solution. It is based on the Stern–Volmer equation, $\phi_{f,0}/\phi_f = 1 + \tau_0 k_Q[Q]$.

☐ 14. Collisional deactivation, electron transfer, and resonance energy transfer are common fluorescence quenching processes. The rate constants of electron and resonance energy transfer decrease with increasing separation between donor and acceptor molecules.

☐ 15. In photosensitization, the reaction of a molecule that does not absorb radiation directly is made to occur by energy transfer during a collision with a molecule that does absorb radiation.

Further reading

Articles and texts

J. Andraos, How mathematics figures in chemistry: some examples. *J. Chem. Educ.* **76**, 258 (1999).

C.E. Carraher, Jr., *Seymour/Carraher's polymer chemistry*, Marcel Dekker (2000).

A. Fersht, *Structure and mechanism in protein science: a guide to enzyme catalysis and protein folding*. W.H. Freeman, New York (1999).

A.M. Kuznetsov and J. Ulstrup, *Electron transfer in chemistry and biology: an introduction to the theory*. Wiley, New York (1998).

J.I. Steinfeld, J.S. Francisco, and W.L. Hase, *Chemical kinetics and dynamics*. Prentice Hall, Englewood Cliffs (1998).

N.J. Turro, *Modern molecular photochemistry*. University Science Books, Sausalito (1991).

K.E. van Holde, W.C. Johnson and P.H. Ho, *Principles of physical biochemistry*. Prentice Hall, Upper Saddle River (1998).

D. Voet and J.G. Voet, *Biochemistry*. Wiley, New York (2004).

Sources of data and information

D.R. Lide (ed.), *CRC handbook of chemistry and physics*, Section 5. CRC Press, Boca Raton (2000).

S.L. Murov, I. Carmichael, and G.L. Hug, *Handbook of photochemistry*. Marcel Dekker, New York (1993).

NDRL/NIST solution kinetics database, NIST standard reference database 40, National Institute of Standards and Technology, Gaithersburg (1994). The URL is available on the web site for this book.

NIST chemical kinetics database, NIST standard reference database 17, National Institute of Standards and Technology, Gaithersburg (1998). The URL is available on the web site for this book.

Further information

Further information 23.1 *The Förster theory of resonance energy transfer*

From the qualitative description given in Section 23.7e, we conclude that resonance energy transfer arises from the interaction between two oscillating dipoles with moments μ_S and μ_Q. From Section 18.4, the energy of the dipole–dipole interaction, $V_{\text{dipole–dipole}}$, is

$$V_{\text{dipole–dipole}} \propto \frac{\mu_S \mu_Q}{R^3}$$

where R is the distance between the dipoles. We saw in Section 9.10 that the rate of a transition from a state i to a state f at a radiation frequency ν is proportional to the square modulus of the matrix element of the perturbation between the two states:

$$w_{f\leftarrow i} \propto |H^{(1)}_{fi}|^2$$

For energy transfer, the wavefunctions of the initial and final states may be denoted as $\psi_S^* \psi_Q$ and $\psi_S \psi_Q^*$, respectively, and $H^{(1)}$ may be written from $V_{\text{dipole–dipole}}$. It follows that the rate of energy transfer, w_T, at a fixed distance R is given (using notation introduced in *Further information 9.1*) by

$$w_T \propto \frac{1}{R^6} \left| \left\langle \psi_S \psi_{Q^*} \middle| \mu_S \mu_Q \middle| \psi_{S^*} \psi_Q \right\rangle \right|^2$$

$$= \frac{1}{R^6} \left| \left\langle \psi_S \middle| \mu_S \middle| \psi_{S^*} \right\rangle \right|^2 \left| \left\langle \psi_{Q^*} \middle| \mu_Q \middle| \psi_Q \right\rangle \right|^2$$

We have used the fact that the terms related to S are functions of coordinates that are independent of those for the functions related to Q. In the last expression, the integrals are squares of transition dipole moments at the radiation frequency ν, the first

corresponding to emission of S* to S and the second to absorption of Q to Q*.

We interpret the expression for w_T as follows. The rate of energy transfer is proportional to R^{-6}, so it decreases sharply with increasing separation between the energy donor and acceptor. Furthermore, the energy transfer rate is optimized when both emission of radiation by S* and absorption of radiation by Q are efficient at the frequency ν. Because the absorption and emission spectra of large molecules in condensed phases are broad, it follows that the energy transfer rate is optimal at radiation frequencies in which the emission spectrum of the donor and the absorption spectrum of the acceptor overlap significantly.

In practice, it is more convenient to measure the efficiency of energy transfer and not the rate itself. In much the same way that we defined the quantum yield as a ratio of rates, we can also define the efficiency of energy transfer, E_T, as the ratio

$$E_T = \frac{w_T}{w_T + w_0} \qquad w_0 = (k_f + k_{IC} + k_{ISC})[S^*] \tag{23.40}$$

where w_0 is the rate of deactivation of S* in the absence of the quencher. The efficiency, E_T, may be expressed in terms of the experimental fluorescence quantum yields $\varphi_{f,0}$ and φ_f of the donor in the absence and presence of the acceptor, respectively. To proceed, we use eqn 23.30 to write:

$$\phi_{f,0} = \frac{v_f}{w_0} \qquad \text{and} \qquad \phi_f = \frac{v_f}{w_0 + w_T}$$

where v_f is the rate of fluorescence. Subsituting these results into eqn 23.40 gives, after a little algebra, eqn 23.37.

Alternatively, we can express w_0 in terms of the parameter R_0, the characteristic distance at which $w_T = w_0$ for a specified pair of S and Q (Table 23.3). By using $w_T \propto R^{-6}$ and $w_0 \propto R_0^{-6}$, we can rearrange the expression for E_T into eqn 23.38.

Discussion questions

23.1 Identify any initiation, propagation, retardation, inhibition, and termination steps in the following chain mechanisms:

(a) (1) $AH \rightarrow A\cdot + H\cdot$
(2) $A\cdot \rightarrow B\cdot + C$
(3) $AH + B\cdot \rightarrow A\cdot + D$
(4) $A\cdot + B\cdot \rightarrow P$

(b) (1) $A_2 \rightarrow A\cdot + A\cdot$
(2) $A\cdot \rightarrow B\cdot + C$
(3) $A\cdot + P \rightarrow B\cdot$
(4) $A\cdot + B\cdot \rightarrow P$

23.2 Bearing in mind distinctions between the mechanisms of stepwise and chain polymerization, describe ways in which it is possible to control the molar mass of a polymer by manipulating the kinetic parameters of polymerization.

23.3 Discuss the features, advantages, and limitations of the Michaelis–Menten mechanism of enzyme action.

23.4 Distinguish between competitive, non-competitive, and uncompetitive inhibition of enzymes. Discuss how these modes of inhibition may be detected experimentally.

23.5 Distinguish between the primary quantum yield and overall quantum yield of a chemical reaction. Describe an experimental procedure for the determination of the quantum yield.

23.6 Discuss experimental procedures that make it possible to differentiate between quenching by energy transfer, collisions, or electron transfer.

23.7 Summarize the main features of the Förster theory of resonance energy transfer. Then, discuss FRET in terms of Förster theory.

Exercises

In the following exercises and problems, it is recommended that rate constants are labelled with the number of the step in the proposed reaction mechanism, and any reverse steps are labelled similarly but with a prime.

23.1a Derive the rate law for the decomposition of ozone in the reaction $2\,O_3(g) \rightarrow 3\,O_2(g)$ on the basis of the following proposed mechanism:

(1) $O_3 \rightleftharpoons O_2 + O$ $\quad k_1, k_1'$
(2) $O + O_3 \rightarrow O_2 + O_2$ $\quad k_2$

23.1b On the basis of the following proposed mechanism, account for the experimental fact that the rate law for the decomposition $2\,N_2O_5(g) \rightarrow 4\,NO_2(g) + O_2(g)$ is $v = k[N_2O_5]$.

(1) $N_2O_5 \rightleftharpoons NO_2 + NO_3$ $\quad k_1, k_1'$
(2) $NO_2 + NO_3 \rightarrow NO_2 + O_2 + NO$ $\quad k_2$
(3) $NO + N_2O_5 \rightarrow NO_2 + NO_2 + NO_2$ $\quad k_3$

23.2a A slightly different mechanism for the decomposition of N_2O_5 from that in Exercise 23.1b has also been proposed. It differs only in the last step, which is replaced by

(3) $NO + NO_3 \rightarrow NO_2 + NO_2$ $\quad k_3$

Show that this mechanism leads to the same overall rate law.

23.2b Consider the following mechanism for the thermal decomposition of R_2:

(1) $R_2 \rightarrow R + R$
(2) $R + R_2 \rightarrow P_B + R'$
(3) $R' \rightarrow P_A + R$
(4) $R + R \rightarrow P_A + P_B$

where R_2, P_A, P_B are stable hydrocarbons and R and R′ are radicals. Find the dependence of the rate of decomposition of R_2 on the concentration of R_2.

23.3a Refer to Fig. 23.3 and determine the pressure range for a branching chain explosion in the hydrogen–oxygen reaction at 800 K.

23.3b Refer to Fig. 23.3 and determine the pressure range for a branching chain explosion in the hydrogen–oxygen reaction at (a) 700 K, (b) 900 K.

23.4a The condensation reaction of propanone, $(CH_3)_2CO$, in aqueous solution is catalysed by bases, B, which react reversibly with propanone to form the carbanion $C_3H_5O^-$. The carbanion then reacts with a molecule of propanone to give the product. A simplified version of the mechanism is

(1) $AH + B \rightarrow BH^+ + A^-$

(2) $A^- + BH^+ \rightarrow AH + B$

(3) $A^- + AH \rightarrow$ product

where AH stands for propanone and A^- denotes its carbanion. Use the steady-state approximation to find the concentration of the carbanion and derive the rate equation for the formation of the product.

23.4b Consider the acid-catalysed reaction

(1) $HA + H^+ \rightleftharpoons HAH^+$ k_1k_1', both fast

(2) $HAH^+ + B \rightarrow BH^+ + AH$ k_2, slow

Deduce the rate law and show that it can be made independent of the specific term $[H^+]$.

23.5a Consider the following chain mechanism:

(1) $AH \rightarrow A\cdot + H\cdot$

(2) $A\cdot \rightarrow B\cdot + C$

(3) $AH + B\cdot \rightarrow A\cdot + D$

(4) $A\cdot + B\cdot \rightarrow P$

Use the steady-state approximation to deduce that the decomposition of AH is first-order in AH.

23.5b Consider the following chain mechanism:

(1) $A_2 \rightarrow A\cdot + A\cdot$

(2) $A\cdot \rightarrow B\cdot + C$

(3) $A\cdot + P \rightarrow B\cdot$

(4) $A\cdot + B\cdot \rightarrow P$

Use the steady-state approximation to deduce that the rate law for the consumption of A_2.

23.6a The enzyme-catalysed conversion of a substrate at 25°C has a Michaelis constant of 0.035 mol dm^{-3}. The rate of the reaction is 1.15×10^{-3} mol dm^{-3} s^{-1} when the substrate concentration is 0.110 mol dm^{-3}. What is the maximum velocity of this enzymolysis?

23.6b The enzyme-catalysed conversion of a substrate at 25°C has a Michaelis constant of 0.042 mol dm^{-3}. The rate of the reaction is 2.45×10^{-4} mol dm^{-3} s^{-1} when the substrate concentration is 0.890 mol dm^{-3}. What is the maximum velocity of this enzymolysis?

23.7a In a photochemical reaction $A \rightarrow 2\,B + C$, the quantum efficiency with 500 nm light is 2.1×10^2 mol einstein^{-1} (1 einstein = 1 mol photons). After exposure of 300 mmol of A to the light, 2.28 mmol of B is formed. How many photons were absorbed by A?

23.7b In a photochemical reaction $A \rightarrow B + C$, the quantum efficiency with 500 nm light is 1.2×10^2 mol einstein^{-1}. After exposure of 200 mmol A to the light, 1.77 mmol B is formed. How many photons were absorbed by A?

23.8a In an experiment to measure the quantum efficiency of a photochemical reaction, the absorbing substance was exposed to 490 nm light from a 100 W source for 45 min. The intensity of the transmitted light was 40 per cent of the intensity of the incident light. As a result of irradiation, 0.344 mol of the absorbing substance decomposed. Determine the quantum efficiency.

23.8b In an experiment to measure the quantum efficiency of a photochemical reaction, the absorbing substance was exposed to 320 nm radiation from a 87.5 W source for 28.0 min. The intensity of the transmitted light was 0.257 that of the incident light. As a result of irradiation, 0.324 mol of the absorbing substance decomposed. Determine the quantum efficiency.

Problems*

Numerical problems

23.1 Studies of combustion reactions depend on knowing the concentrations of H atoms and HO radicals. Measurements on a flow system using EPR for the detection of radicals gave information on the reactions

(1) $H + NO_2 \rightarrow OH + NO$ $k_1 = 2.9 \times 10^{10}$ dm^3 mol^{-1} s^{-1}

(2) $OH + OH \rightarrow H_2O + O$ $k_2 = 1.55 \times 10^9$ dm^3 mol^{-1} s^{-1}

(3) $O + OH \rightarrow O_2 + H$ $k_3 = 1.1 \times 10^{10}$ dm^3 mol^{-1} s^{-1}

(J.N. Bradley, W. Hack, K. Hoyermann, and H.G. Wagner, *J. Chem. Soc. Faraday Trans.* I, 1889 (1973)). Using initial H atom and NO_2 concentrations of 4.5×10^{-10} mol cm^{-3} and 5.6×10^{-10} mol cm^{-3}, respectively, compute and plot curves showing the O, O_2, and OH concentrations as a function of time in the range 0–10 ns.

23.2 In a flow study of the reaction between O atoms and Cl_2 (J.N. Bradley, D.A. Whytock, and T.A. Zaleski, *J. Chem. Soc. Faraday Trans.* I, 1251 (1973)) at high chlorine pressures, plots of $\ln [O]_0/[O]$ against distances l along the flow tube, where $[O]_0$ is the oxygen concentration at zero chlorine pressure, gave straight lines. Given the flow velocity as 6.66 m s^{-1} and the data below, find the rate coefficient for the reaction $O + Cl_2 \rightarrow ClO + Cl$.

l/cm	0	2	4	6	8	10	12	14	16	18
$\ln([O]_0/[O])$	0.27	0.31	0.34	0.38	0.45	0.46	0.50	0.55	0.56	0.60

with $[O]_0 = 3.3\ 10^{-8}$ mol dm^{-3}, $[Cl_2] = 2.54 \times 10^{-7}$ mol dm^{-3}, $p = 1.70$ Torr.

23.3‡ J.D. Chapple-Sokol, C.J. Giunta, and R.G. Gordon (*J. Electrochem. Soc.* **136**, 2993 (1989)) proposed the following radical chain mechanism for the initial stages of the gas-phase oxidation of silane by nitrous oxide:

(1) $N_2O \rightarrow N_2 + O$

(2) $O + SiH_4 \rightarrow SiH_3 + OH$

(3) $OH + SiH_4 \rightarrow SiH_3 + H_2O$

(4) $SiH_3 + N_2O \rightarrow SiH_3O + N_2$

* Problems denoted with the symbol ‡ were supplied by Charles Trapp, Carmen Giunta, and Marshall Cady.

(5) $SiH_3O + SiH_4 \rightarrow SiH_3OH + SiH_3$

(6) $SiH_3 + SiH_3O \rightarrow (H_3Si)_2O$

Label each step with its role in the chain. Use the steady-state approximation to show that this mechanism predicts the following rate law for SiH_4 consumption (provided k_1 and k_6 are in some sense small):

$$\frac{d[SiH_4]}{dt} = -k[N_2O][SiH_4]^{1/2}$$

23.4‡ The water formation reaction has been studied many times and continues to be of interest. Despite the many studies there is not uniform agreement on the mechanism. But as explosions are known to occur at certain critical values of the pressure, any proposed mechanism to be considered plausible must be consistent with the existence of these critical explosion limits. One such plausible mechanism is that of Example 23.2. Another is the following:

(1) $H_2 \rightarrow H + H$

(2) $H + O_2 \rightarrow OH + O$

(3) $O + H_2 \rightarrow OH + H$

(4) $H + O_2 \rightarrow HO_2$

(5) $HO_2 + H_2 \rightarrow H_2O + OH$

(6) $HO_2 + \text{wall} \rightarrow \text{destruction}$

(7) $H + M \rightarrow \text{destruction}$

In a manner similar to that in Example 23.2, determine whether or not this mechanism can lead to explosions under appropriate conditions.

23.5‡ For many years the reaction $H_2(g) + I_2(g) \rightarrow 2\,HI(g)$ and its reverse were assumed to be elementary bimolecular reactions. However, J.H. Sullivan (*J. Chem. Phys.* **46**, 73 (1967)) suggested that the following mechanism for the reaction, originally proposed by M. Bodenstein (*Z. Physik. Chem.* **29**, 56 (1898)), provides a better explanation of the experimental results:

(1) $I_2 \rightleftharpoons I + I$ $\quad k_1, k_1'$

(2) $I + I + H_2 \rightarrow HI + HI$ $\quad k_2$

Obtain the expression for the rate of formation of HI based on this mechanism. Under what conditions does this rate law reduce to the one for the originally accepted mechanism?

23.6 The number of photons falling on a sample can be determined by a variety of methods, of which the classical one is chemical actinometry. The decomposition of oxalic acid $(COOH)_2$, in the presence of uranyl sulfate, $(UO_2)SO_4$, proceeds according to the sequence

(1) $UO^{2+} + h\nu \rightarrow (UO^{2+})^*$

(2) $(UO^{2+})^* + (COOH)_2 \rightarrow UO^{2+} + H_2O + CO_2 + CO$

with a quantum efficiency of 0.53 at the wavelength used. The amount of oxalic acid remaining after exposure can be determined by titration (with $KMnO_4$) and the extent of decomposition used to find the number of incident photons. In a particular experiment, the actinometry solution consisted of 5.232 g anhydrous oxalic acid, 25.0 cm^3 water (together with the uranyl salt). After exposure for 300 s the remaining solution was titrated with 0.212 M $KMnO_4(aq)$, and 17.0 cm^3 were required for complete oxidation of the remaining oxalic acid. The titration reaction is

$$2\,MnO_4^-(aq) + 5\,(COOH)_2(aq) + 6\,H^+(aq) \rightarrow 10\,CO_2(g) + 8\,H_2O(l) + 2\,Mn^{2+}(aq)$$

What is the rate of incidence of photons at the wavelength of the experiment? Express the answer in photons/second and einstein/second.

23.7 Dansyl chloride, which absorbs maximally at 330 nm and fluoresces maximally at 510 nm, can be used to label aminoacids in fluorescence microscopy and FRET studies. Tabulated below is the variation of the fluorescence intensity of an aqueous solution of dansyl chloride with time after excitation by a short laser pulse (with I_0 the initial fluorescence intensity).

t/ns	5.0	10.0	15.0	20.0
I_f/I_0	0.45	0.21	0.11	0.05

(a) Calculate the observed fluorescence lifetime of dansyl chloride in water. (b) The fluorescence quantum yield of dansyl chloride in water is 0.70. What is the fluorescence rate constant?

23.8 When benzophenone is illuminated with ultraviolet light it is excited into a singlet state. This singlet changes rapidly into a triplet, which phosphoresces. Triethylamine acts as a quencher for the triplet. In an experiment in methanol as solvent, the phosphorescence intensity varied with amine concentration as shown below. A time-resolved laser spectroscopy experiment had also shown that the half-life of the fluorescence in the absence of quencher is 29 μs. What is the value of k_q?

[Q]/(mol dm^{-3})	0.0010	0.0050	0.0100
I_f/(arbitrary units)	0.41	0.25	0.16

23.9 An electronically excited state of Hg can be quenched by N_2 according to

$$Hg^*(g) + N_2(g, v = 0) \rightarrow Hg(g) + N_2(g, v = 1)$$

in which energy transfer from Hg^* excites N_2 vibrationally. Fluorescence lifetime measurements of samples of Hg with and without N_2 present are summarized below ($T = 300$ K):

$p_{N_2} = 0.0$ atm					
Relative fluorescence intensity	1.000	0.606	0.360	0.22	0.135
t/μs	0.0	5.0	10.0	15.0	20.0
$p_{N_2} = 9.74 \times 10^{-4}$ atm					
Relative fluorescence intensity	1.000	0.585	0.342	0.200	0.117
t/μs	0.0	3.0	6.0	9.0	12.0

You may assume that all gases behave ideally. Determine the rate constant for the energy transfer process.

23.10 The Förster theory of resonance energy transfer and the basis for the FRET technique can be tested by performing fluorescence measurements on a series of compounds in which an energy donor and an energy acceptor are covalently linked by a rigid molecular linker of variable and known length. L. Stryer and R.P. Haugland (*Proc. Natl. Acad. Sci. USA* **58**, 719 (1967)) collected the following data on a family of compounds with the general composition dansyl-(L-prolyl)$_n$-naphthyl, in which the distance R between the naphthyl donor and the dansyl acceptor was varied from 1.2 nm to 4.6 nm by increasing the number of prolyl units in the linker:

R/nm	1.2	1.5	1.8	2.8	3.1	3.4	3.7	4.0	4.3	4.6
$1 - E_T$	0.99	0.94	0.97	0.82	0.74	0.65	0.40	0.28	0.24	0.16

Are the data described adequately by eqn 23.38? If so, what is the value of R_0 for the naphthyl-dansyl pair?

Theoretical problems

23.11 The Rice–Herzfeld mechanism for the dehydrogenation of ethane is specified in Section 23.1, and it was noted there that it led to first-order kinetics. Confirm this remark, and find the approximations that lead to the rate law quoted there. How may the conditions be changed so that the reaction shows different orders?

23.12 The following mechanism has been proposed for the thermal decomposition of acetaldehyde (ethanal):

(1) $CH_3CHO \rightarrow \cdot CH_3 + CHO$

(2) $\cdot CH_3 + CH_3CHO \rightarrow CH_4 + \cdot CH_2CHO$

(3) $\cdot CH_2CHO \rightarrow CO + \cdot CH_3$

(4) $\cdot CH_3 + \cdot CH_3 \rightarrow CH_3CH_3$

Find an expression for the rate of formation of methane and the rate of disappearance of acetaldehyde.

23.13 Express the root mean square deviation $\{\langle M^2\rangle - \langle M\rangle^2\}^{1/2}$ of the molar mass of a condensation polymer in terms of p, and deduce its time dependence.

23.14 Calculate the ratio of the mean cube molar mass to the mean square molar mass in terms of (a) the fraction p, (b) the chain length.

23.15 Calculate the average polymer length in a polymer produced by a chain mechanism in which termination occurs by a disproportionation reaction of the form $M\cdot + \cdot M \rightarrow M + :M$.

23.16 Derive an expression for the time dependence of the degree of polymerization for a stepwise polymerization in which the reaction is acid-catalysed by the —COOH acid functional group. The rate law is $d[A]/dt = -k[A]^2[OH]$.

23.17 Autocatalysis is the catalysis of a reaction by the products. For example, for a reaction A → P it may be found that the rate law is $v = k[A][P]$ and the reaction rate is proportional to the concentration of P. The reaction gets started because there are usually other reaction routes for the formation of some P initially, which then takes part in the autocatalytic reaction proper. (a) Integrate the rate equation for an autocatalytic reaction of the form A → P, with rate law $v = k[A][P]$, and show that

$$\frac{[P]}{[P]_0} = (b+1)\frac{e^{at}}{1+be^{at}}$$

where $a = ([A]_0 + [P]_0)k$ and $b = [P]_0/[A]_0$. *Hint*. Starting with the expression $v = -d[A]/dt = k[A][P]$, write $[A] = [A]_0 - x$, $[P] = [P]_0 + x$ and then write the expression for the rate of change of either species in terms of x. To integrate the resulting expression, the following relation will be useful:

$$\frac{1}{([A]_0 - x)([P]_0 + x)} = \frac{1}{[A]_0 + [P]_0}\left(\frac{1}{[A]_0 - x} + \frac{1}{[P]_0 + x}\right)$$

(b) Plot $[P]/[P]_0$ against at for several values of b. Discuss the effect of autocatalysis on the shape of a plot of $[P]/[P]_0$ against t by comparing your results with those for a first-order process, in which $[P]/[P]_0 = 1 - e^{-kt}$. (c) Show that, for the autocatalytic process discussed in parts (a) and (b), the reaction rate reaches a maximum at $t_{max} = -(1/a)\ln b$. (d) An autocatalytic reaction A → P is observed to have the rate law $d[P]/dt = k[A]^2[P]$. Solve the rate law for initial concentrations $[A]_0$ and $[P]_0$. Calculate the time at which the rate reaches a maximum. (e) Another reaction with the stoichiometry A → P has the rate law $d[P]/dt = k[A][P]^2$; integrate the rate law for initial concentrations $[A]_0$ and $[P]_0$. Calculate the time at which the rate reaches a maximum.

23.18 Conventional equilibrium considerations do not apply when a reaction is being driven by light absorption. Thus the steady-state concentration of products and reactants might differ significantly from equilibrium values. For instance, suppose the reaction A → B is driven by light absorption and that its rate is I_a, but that the reverse reaction B → A is bimolecular and second-order with a rate $k[B]^2$. What is the stationary state concentration of B? Why does this 'photostationary state' differ from the equilibrium state?

23.19 Derive an expression for the rate of disappearance of a species A in a photochemical reaction for which the mechanism is:

(1) initiation with light of intensity I, $A \rightarrow R\cdot + R\cdot$

(2) propagation, $A + R\cdot \rightarrow R\cdot + B$

(3) termination, $R\cdot + R\cdot \rightarrow R_2$

Hence, show that rate measurements will give only a combination of k_2 and k_3 if a steady state is reached, but that both may be obtained if a steady state is not reached.

23.20 The photochemical chlorination of chloroform in the gas has been found to follow the rate law $d[CCl_4]/dt = k[Cl_2]^{1/2}I_a^{1/2}$. Devise a mechanism that leads to this rate law when the chlorine pressure is high.

23.21 Photolysis of $Cr(CO)_6$ in the presence of certain molecules M, can give rise to the following reaction sequence:

(1) $Cr(CO)_6 + h\nu \rightarrow Cr(CO)_5 + CO$

(2) $Cr(CO)_5 + CO \rightarrow Cr(CO)_6$

(3) $Cr(CO)_5 + M \rightarrow Cr(CO)_5M$

(4) $Cr(CO)_5M \rightarrow Cr(CO)_5 + M$

Suppose that the absorbed light intensity is so weak that $I \ll k_4[Cr(CO)_5M]$. Find the factor f in the equation $d[Cr(CO)_5M]/dt = -f[Cr(CO)_5M]$. Show that a graph of $1/f$ against $[M]$ should be a straight line.

Applications: to biochemistry and environmental science

23.22 Models of population growth are analogous to chemical reaction rate equations. In the model due to Malthus (1798) the rate of change of the population N of the planet is assumed to be given by dN/dt = births − deaths. The numbers of births and deaths are proportional to the population, with proportionality constants b and d. Obtain the integrated rate law. How well does it fit the (very approximate) data below on the population of the planet as a function of time?

Year	1750	1825	1922	1960	1974	1987	2000
$N/10^9$	0.5	1	2	3	4	5	6

23.23 Many enzyme-catalysed reactions are consistent with a modified version of the Michaelis–Menten mechanism in which the second step is also reversible. (a) For this mechanism show that the rate of formation of product is given by

$$v = \frac{(v_{max}/K_M)[S] - (v'_{max}/K'_M)[P]}{1 + [S]/K_M + [P]/K'_M}$$

where $v_{max} = k_b[E]_0$, $v'_{max} = k'_a[E]_0$, $K_M = (k'_a + k_b)/k_a$, and, and $K'_M = (k'_a + k_b)/k'_b$. (b) Find the limiting behaviour of this expression for large and small concentrations of substrate.

23.24 The following results were obtained for the action of an ATPase on ATP at 20°C, when the concentration of the ATPase was 20 nmol dm^{-3}:

[ATP]/(μmol dm^{-3})	0.60	0.80	1.4	2.0	3.0
v/(μmol dm^{-3} s^{-1})	0.81	0.97	1.30	1.47	1.69

Determine the Michaelis constant, the maximum velocity of the reaction, the turnover number, and the catalytic efficiency of the enzyme.

23.25 Enzyme-catalysed reactions are sometimes analysed by use of the *Eadie–Hofstee plot*, in which v is plotted against $v/[S]_0$. (a) Using the simple Michaelis–Menten mechanism, derive a relation between $v/[S]_0$ and v. (b) Discuss how the values of K_M and v_{max} are obtained from analysis of the Eadie–Hofstee plot. (c) Determine the Michaelis constant and the maximum velocity of the reaction of the reaction from Exercise 23.23 by using an Eadie–Hofstee plot to analyse the data.

23.26 In general, the catalytic efficiency of an enzyme depends on the pH of the medium in which it operates. One way to account for this behaviour is to propose that the enzyme and the enzyme–substrate complex are active only in specific protonation states. This situation can be summarized by the following mechanism:

$$EH + S \Leftrightarrow ESH \qquad k_a, k'_a$$
$$ESH \rightarrow E + P \qquad k_b$$
$$EH \rightleftharpoons E^- + H^+ \qquad K_{E,a} = \frac{[E^-][H^+]}{[EH^+]}$$
$$EH_2^+ \rightleftharpoons EH + H^+ \qquad K_{E,b} = \frac{[EH][H^+]}{[EH_2^+]}$$
$$ESH \rightleftharpoons ES^- + H^+ \qquad K_{ES,a} = \frac{[ES^-][H^+]}{[ESH]}$$
$$ESH_2 \rightleftharpoons ESH + H^+ \qquad K_{ES,b} = \frac{[ESH][H^+]}{[ESH_2]}$$

in which only the EH and ESH forms are active. (a) For the mechanism above, show that

$$v = \frac{v'_{max}}{1 + K'_M[S]_0}$$

with

$$v'_{max} = \frac{v_{max}}{1 + \dfrac{[H^+]}{K_{ES,b}} + \dfrac{K_{ES,a}}{[H^+]}}$$

$$K'_M = K_M \frac{1 + \dfrac{[H^+]}{K_{E,b}} + \dfrac{K_{E,a}}{[H^+]}}{1 + \dfrac{[H^+]}{K_{ES,b}} + \dfrac{K_{ES,a}}{[H^+]}}$$

where v_{max} and K_M correspond to the form EH of the enzyme. (b) For pH values ranging from 0 to 14, plot v'_{max} against pH for a hypothetical reaction for which $v_{max} = 1.0 \times 10^{-6}$ mol dm^{-3} s^{-1}, $K_{ES,b} = 1.0 \times 10^{-6}$ mol dm^{-3} and $K_{ES,a} = 1.0 \times 10^{-8}$ mol dm^{-3}. Is there a pH at which v'_{max} reaches a maximum value? If so, determine the pH. (c) Redraw the plot in part (b) by using the same value of v_{max}, but $K_{ES,b} = 1.0 \times 10^{-4}$ mol dm^{-3} and $K_{ES,a} = 1.0 \times 10^{-10}$ mol dm^{-3}. Account for any differences between this plot and the plot from part (b).

23.27 The enzyme carboxypeptidase catalyses the hydrolysis of polypeptides and here we consider its inhibition. The following results were obtained when the rate of the enzymolysis of carbobenzoxy-glycyl-D-phenylalanine (CBGP) was monitored without inhibitor:

$[CBGP]_0/(10^{-2}$ mol dm$^{-3})$	1.25	3.84	5.81	7.13
Relative reaction rate	0.398	0.669	0.859	1.000

(All rates in this problem were measured with the same concentration of enzyme and are relative to the rate measured when $[CBGP]_0 = 0.0713$ mol dm^{-3} in the absence of inhibitor.) When 2.0×10^{-3} mol dm^{-3} phenylbutyrate ion was added to a solution containing the enzyme and substrate, the following results were obtained:

$[CBGP]_0/(10^{-2}$ mol dm$^{-3})$	1.25	2.50	4.00	5.50
Relative reaction rate	0.172	0.301	0.344	0.548

In a separate experiment, the effect of 5.0×10^{-2} mol dm^{-3} benzoate ion was monitored and the results were:

$[CBGP]_0/(10^{-2}$ mol dm$^{-3})$	1.75	2.50	5.00	10.00
Relative reaction rate	0.183	0.201	0.231	0.246

Determine the mode of inhibition of carboxypeptidase by the phenylbutyrate ion and benzoate ion.

23.28 Many biological and biochemical processes involve autocatalytic steps (Problem 23.17). In the SIR model of the spread and decline of infectious diseases the population is divided into three classes; the susceptibles, S, who can catch the disease, the infectives, I, who have the disease and can transmit it, and the removed class, R, who have either had the disease and recovered, are dead, or are immune or isolated. The model mechanism for this process implies the following rate laws:

$$\frac{dS}{dt} = -rSI \qquad \frac{dI}{dt} = rSI - aI \qquad \frac{dR}{dt} = aI$$

What are the autocatalytic steps of this mechanism? Find the conditions on the ratio a/r that decide whether the disease will spread (an epidemic) or die out. Show that a constant population is built into this system, namely, that S + I + R = N, meaning that the timescales of births, deaths by other causes, and migration are assumed large compared to that of the spread of the disease.

23.29 In light-harvesting complexes, the fluorescence of a chlorophyll molecule is quenched by nearby chlorophyll molecules. Given that for a pair of chlorophyll *a* molecules $R_0 = 5.6$ nm, by what distance should two chlorophyll *a* molecules be separated to shorten the fluorescence lifetime from 1 ns (a typical value for monomeric chlorophyll *a* in organic solvents) to 10 ps?

23.30 The light-induced electron transfer reactions in photosynthesis occur because chlorophyll molecules (whether in monomeric or dimeric forms) are better reducing agents in their electronic excited states. Justify this observation with the help of molecular orbital theory.

23.31 The emission spectrum of a porphyrin dissolved in O_2-saturated water shows a strong band at 650 nm and a weak band at 1270 nm. In separate experiments, it was observed that the electronic absorption spectrum of the porphyrin sample showed bands at 420 nm and 550 nm, and the electronic absorption spectrum of O_2-saturated water showed no bands in the visible range of the spectrum (and therefore no emission spectrum when excited in the same range). Based on these data alone, make a preliminary assignment of the emission band at 1270 nm. Propose additional experiments that test your hypothesis.

23.32‡ Ultraviolet radiation photolyses O_3 to O_2 and O. Determine the rate at which ozone is consumed by 305 nm radiation in a layer of the stratosphere of thickness 1 km. The quantum efficiency is 0.94 at 220 K, the concentration about 8×10^{-9} mol dm^{-3}, the molar absorption coefficient 260 dm^3 mol^{-1} cm^{-1}, and the flux of 305 nm radiation about 1×10^{14} photons cm^{-2} s^{-1}. Data from W.B. DeMore, S.P. Sander, D.M. Golden, R.F. Hampson, M.J. Kurylo, C.J. Howard, A.R. Ravishankara, C.E. Kolb, and M.J. Molina, *Chemical kinetics and photochemical data for use in stratospheric modeling: Evaluation Number 11*, JPL Publication 94–26 (1994).

23.33‡ Use the Chapman model to explore the behaviour of a model atmosphere consisting of pure O_2 at 10 Torr and 298 K that is exposed to measurable frequencies and intensities of UV radiation. (a) Look up the values of k_2, k_4, and k_5 in a source such as the *CRC Handbook of chemistry and physics* or *Chemical kinetics and photochemical data for use in stratospheric modeling* (the URL is available at the text's web site). The rate constants k_1 and k_3 depend upon the radiation conditions; assume values of 1.0×10^{-8} s^{-1} and 0.016 s^{-1}, respectively. If you cannot find a value for k_5, formulate chemically sound arguments for exclusion of the fifth step from the mechanism. (b) Write the rate expressions for the concentration of each chemical species. (c) Assume that the UV radiation is turned on at $t = 0$, and solve the rate expressions for the concentration of all species as a function of time over a period of 4 h. Examine relevant concentrations in the very early time period $t < 0.1$ s. State all assumptions. Is there any ozone present initially? Why must the pressure be low and the UV radiation intensities high for the production of ozone? Draw graphs of the time variations of both atomic oxygen and ozone on both the very short and the long timescales. What is the percentage of ozone after 4.0 h of irradiation? *Hint*. You will need a software package for solving a 'stiff' system of differential equations. Stiff differential equations have at least two rate constants with very different values and result in different behaviours on different timescales, so the solution usually requires that the total time period be broken into two or more periods; one may be

very short and another very long. For help with using mathematical software to solve systems of differential equations, see M.P. Cady and C.A. Trapp, *A Mathcad primer for physical chemistry*. Oxford University Press (1999).

23.34‡ Chlorine atoms react rapidly with ozone in the gas-phase bimolecular reaction $Cl + O_3 \rightarrow ClO + O_2$ with $k = (1.7 \times 10^{10}\ dm^3\ mol^{-1}\ s^{-1})e^{-260/(T/K)}$ (W.B. DeMore, S.P. Sander, D.M. Golden, R.F. Hampson, M.J. Kurylo, C.J. Howard, A.R. Ravishankara, C.E. Kolb, and M.J. Molina, Chemical kinetics and photochemical data for use in stratospheric modeling: Evaluation Number 11, JPL Publication 94–26 (1994)). Estimate the rate of this reaction at (a) 20 km, where $[Cl] = 5 \times 10^{-17}$ mol dm^{-3}, $[O_3] = 8 \times 10^{-9}$ mol dm^{-3}, and $T = 220$ K; (b) 45 km, where $[Cl] = 3 \times 10^{-15}$ mol dm^{-3}, $[O_3] = 8 \times 10^{-11}$ mol dm^{-3}, and $T = 270$ K.

23.35‡ Because of its importance in atmospheric chemistry, the thermal decomposition of nitric oxide, $2\ NO(g) \rightarrow N_2(g) + O_2(g)$, has been amongst the most thoroughly studied of gas-phase reactions. The commonly accepted mechanism has been that of H. Wise and M.F. Freech (*J. Chem. Phys.* **22**, 1724 (1952)):

(1) $NO + NO \rightarrow N_2O + O$ k_1
(2) $O + NO \rightarrow O_2 + N$ k_2
(3) $N + NO \rightarrow N_2 + O$ k_3
(4) $O + O + M \rightarrow O_2 + M$ k_4
(5) $O_2 + M \rightarrow O + O + M$ k_4'

(a) Label the steps of this mechanism as initiation, propagation, etc. (b) Write down the full expression for the rate of disappearance of NO. What does this expression for the rate become on the basis of the assumptions that $v_2 = v_3$ when [N] reaches its steady state concentration, that the rate of the propagation step is more rapid than the rate of the initiation step, and that oxygen atoms are in equilibrium with oxygen molecules? (c) Find an expression for the effective activation energy, $E_{a,eff}$, for the overall reaction in terms of the activation energies of the individual steps of the reaction. (d) Estimate $E_{a,eff}$ from the bond energies of the species involved. (e) It has been pointed out by R.J. Wu and C.T. Yeh (*Int. J. Chem. Kinet.* **28**, 89 (1996)) that the reported experimental values of $E_{a,eff}$ obtained by different authors have varied from 253 to 357 kJ mol^{-1}. They suggest that the assumption of oxygen atoms and oxygen molecules being in equilibrium is unwarranted and that the steady-state approximation needs to be applied to the entire mechanism. Obtain the overall rate law based on the steady-state approximation and find the forms that it assumes for low NO conversion (low O_2 concentration). (f) When the reaction conversion becomes significant, Wu and Yeh suggest that two additional elementary steps,

(6) $O_2 + M \rightarrow O + O + M$ k_6
(7) $NO + O_2 \rightarrow O + NO_2$ k_7

start to compete with step (1) as the initiation step. Obtain the rate laws based on these alternative mechanisms and again estimate the apparent activation energies. Is the range of these different theoretically estimated values for $E_{a,eff}$ consistent with the range of values obtained experimentally?